PROCEEDINGS OF SPIE

Fiber Lasers V: Technology, Systems, and Applications

Jes Broeng
Clifford Headley
Editors

21–24 January 2008
San Jose, California, USA

Sponsored by
SPIE

Cosponsored by
IPG Photonics

Published by
SPIE

Volume 6873

Proceedings of SPIE, 0277-786X, v. 6873

SPIE is an international society advancing an interdisciplinary approach to the science and application of light.

The papers included in this volume were part of the technical conference cited on the cover and title page. Papers were selected and subject to review by the editors and conference program committee. Some conference presentations may not be available for publication. The papers published in these proceedings reflect the work and thoughts of the authors and are published herein as submitted. The publisher is not responsible for the validity of the information or for any outcomes resulting from reliance thereon.

Please use the following format to cite material from this book:
Author(s), "Title of Paper," in *Fiber Lasers V: Technology, Systems, and Applications*, edited by Jes Broeng, Clifford Headley III, Proceedings of SPIE Vol. 6873 (SPIE, Bellingham, WA, 2008) Article CID Number.

ISSN 0277-786X
ISBN 9780819470485

Published by
SPIE
P.O. Box 10, Bellingham, Washington 98227-0010 USA
Telephone +1 360 676 3290 (Pacific Time) · Fax +1 360 647 1445
SPIE.org

Copyright © 2008, Society of Photo-Optical Instrumentation Engineers

Copying of material in this book for internal or personal use, or for the internal or personal use of specific clients, beyond the fair use provisions granted by the U.S. Copyright Law is authorized by SPIE subject to payment of copying fees. The Transactional Reporting Service base fee for this volume is $18.00 per article (or portion thereof), which should be paid directly to the Copyright Clearance Center (CCC), 222 Rosewood Drive, Danvers, MA 01923. Payment may also be made electronically through CCC Online at copyright.com. Other copying for republication, resale, advertising or promotion, or any form of systematic or multiple reproduction of any material in this book is prohibited except with permission in writing from the publisher. The CCC fee code is 0277-786X/08/$18.00.

Printed in the United States of America.

Publication of record for individual papers is online in the SPIE Digital Library.

SPIEDigitalLibrary.org

Paper Numbering: Proceedings of SPIE follow an e-First publication model, with papers published first online and then in print and on CD-ROM. Papers are published as they are submitted and meet publication criteria. A unique, consistent, permanent citation identifier (CID) number is assigned to each article at the time of the first publication. Utilization of CIDs allows articles to be fully citable as soon they are published online, and connects the same identifier to all online, print, and electronic versions of the publication. SPIE uses a six-digit CID article numbering system in which:

- The first four digits correspond to the SPIE volume number.
- The last two digits indicate publication order within the volume using a Base 36 numbering system employing both numerals and letters. These two-number sets start with 00, 01, 02, 03, 04, 05, 06, 07, 08, 09, 0A, 0B … 0Z, followed by 10-1Z, 20-2Z, etc.

The CID number appears on each page of the manuscript. The complete citation is used on the first page, and an abbreviated version on subsequent pages. Numbers in the index correspond to the last two digits of the six-digit CID number.

Contents

xi *Conference Committee*

xiii *The long journey from idea to industrial success (Plenary Paper) [6874-26]*
H. Schlüter, TRUMPF Inc. (USA)

Post Deadline Papers

xxix *High power fused pump/signal combiner for reverse pumping of active double clad fibers*
O. Lumholt, S. Agger, T. T. Alkeskjold, K. B. Bing, M. Denninger, T. Nikolajsen, Crystal Fibre A/S (Denmark)

xxxiii *Single-polarization single-transverse-mode rod-type photonic crystal fiber with mode-field-area of 2300 μm²*
O. Schmidt, J. Rothhardt, T. Eidam, F. Röser, J. Limpert, A. Tünnermann, Friedrich-Schiller-Univ. Jena (Germany); K. P. Hansen, C. Jakobsen. J. Broeng, Crystal Fibre A/S (Denmark)

xxxv *Spatially and spectrally resolved imaging of higher-order-modes in large-mode-area fibers*
J. W. Nicholson, A. D. Yablon, OFS Labs. (USA)

xxxvii *High power nanosecond pulse amplification at 2-microns in thulium-doped fiber pumped at 795nm*
D. Creeden, P. A. Budni, P. A. Ketteridge, BAE Systems (USA)

xxxix *Millijoule pulse energy high repetition rate femtosecond fiber CPA system: results, SHG and scaling potential*
F. Röser, J. Rothhardt, T. Eidam, O. Schmidt, D. N. Schimpf, J. Limpert, A. Tünnermann, Friedrich-Schiller-Univ. Jena (Germany)

xliii *100 W femtosecond Yb-fiber CPA system based on chirped-volume-Bragg-gratings*
G. Chang, M. Rever, Univ. of Michigan (USA); V. Smirnov, OptiGrate (USA); L. Glebov, College of Optics and Photonics/CREOL, Univ. of Central Florida (USA); A. Galvanauskas, Univ. of Michigan (USA)

xlv *Stretcher-free high energy nonlinear amplification of femtosecond pulses in rod-type fiber*
Y. Zouter, Ctr. Lasers Intenses et Applications (France) and Amplitude Systèmes (France); D. N. Papadopoulos, M. Hanna, Lab. Charles Fabry de l'Institut d'Optique, Univ. Paris Sud (France); J. Boullet, L. Huang, Ctr. Lasers Intenses et Applications (France); F. Druon, Lab. Charles Fabry de l'Institut d'Optique, Univ. Paris Sud (France); E. Mottay, Amplitude Systèmes (France); P. Georges, Lab. Charles Fabry de l'Institut d'Optique, Univ. Paris Sud (France); E. Cormier, Ctr. Lasers Intenses et Applications (France)

xlix *A novel mode-locked fiber laser based on chirped-pulse oscillator concept*
B. Ortaç, M. Plötner, T. Schreiber, J. Limpert, A. Tünnermann, Friedrich-Schiller-Univ. Jena (Germany)

li *High speed laser micro-machining using a high repetition rate, high average power femotosecond fiber CPA system*
A. Ancona, Friedrich-Schiller-Univ. Jena (Germany) and CNR-INFM Regional Lab (Italy): K. Rademaker, F. Röser, J. Limpert, S. Nolte, Friedrich-Schiller-Univ. Jena (Germany); A. Tünnermann, Friedrich-Schiller-Univ. Jena (Germany) and Fraunhofer Institute for Applied Optics and Precision Engineering IOF (Germany)

FIBER DESIGNS

6873 07 **Airclad fiber laser technology (Invited Paper)** [6873-06]
K. P. Hansen, Crystal Fibre A/S (Denmark); C. B. Olausson, Crystal Fibre A/S (Denmark) and COM-DTU (Denmark); J. Broeng, K. Mattsson, M. D. Nielsen, T. Nikolajsen, P. M. W. Skovgaard, M. H. Sørensen, M. Denninger, C. Jakobsen, H. R. Simonsen, Crystal Fibre A/S (Denmark)

6873 08 **Measurement of bend-induced nonlinearities in large-mode-area fibers** [6873-07]
J. W. Nicholson, J. M. Fini, A. D. Yablon, P. S. Westbrook, K. Feder, C. Headley, OFS Labs. (USA)

6873 0A **Modal sensitivity analysis for single mode operation in large mode area fiber** [6873-09]
B. Sévigny, X. Zhang, M. Garneau, M. Faucher, Y. K. Lizé, N. Holehouse, ITF Labs (Canada)

PULSED SOURCES

6873 0C **50W single-mode linearly polarized high peak power pulsed fiber laser with tunable ns-µs pulse durations and kHz-MHz repetition rates** [6873-11]
V. Khitrov, B. Samson, D. Machewirth, K. Tankala, Nufern (USA)

6873 0D **Q-switched fiber lasers with controlled pulse shape** [6873-12]
J. P. Feve, J. Morehead, S. Makki, J. Franke, M. Muendel, JDSU (USA); C. Wang, G. Zhao, Nufern (USA)

NARROWLINEWIDTH SOURCES AND SBS SUPPRESION

6873 0K **High power Yb-doped fiber laser-based LIDAR for space weather** [6873-19]
C. G. Carlson, P. D. Dragic, B. W. Graf, R. K. Price, J. J. Coleman, G. R. Swenson, Univ. of Illinois at Urbana-Champaign (USA)

6873 0L **All-fiber 194 W single-frequency single-mode Yb-doped master-oscillator power-amplifier** [6873-20]
M. D. Mermelstein, K. Brar, M. J. Andrejco, A. D. Yablon, M. Fishteyn, C. Headley, D. J. DiGiovanni, OFS Labs. (USA)

6873 0N **11.2 dB SBS gain suppression in a large mode area Yb-doped optical fiber** [6873-22]
M. D. Mermelstein, M. J. Andrejco, J. Fini, A. Yablon, C. Headley, D. J. DiGiovanni, OFS Labs. (USA); A. H. McCurdy, Optical Fiber Design Group of OFS (USA)

6873 0O **Suppression of stimulated Brillouin scattering in single-frequency multi-kilowatt fiber amplifiers** [6873-23]
J. E. Rothenberg, P. A. Thielen, M. Wickham, C. P. Asman, Northrop Grumman Space Technology (USA)

FEMTOSECOND LASERS

6873 0P **High-energy femtosecond fiber lasers (Invited Paper)** [6873-24]
A. Chong, W. Renninger, F. W. Wise, Cornell Univ. (USA)

6873 0Q **Optimization of higher order mode fibers for dispersion management of femtosecond fiber lasers** [6873-25]
L. Grüner-Nielsen, OFS Fitel Denmark ApS (Denmark); S. Ramachandran, OFS Labs. (USA); K. Jespersen, OFS Fitel Denmark ApS (Denmark); S. Ghalmi, OFS Labs. (USA); M. Garmund, B. Pálsdóttir, OFS Fitel Denmark ApS (Denmark)

6873 0R **200 nJ pulse energy femtosecond Yb-doped dispersion compensation free fiber oscillator** [6873-26]
B. Ortaç, O. Schmidt, Friedrich-Schiller-Univ. Jena (Germany); T. Schreiber, Fraunhofer Institute for Applied Optics and Precision Engineering (Germany); A. Hideur, Univ. de Rouen (France); J. Limpert, Friedrich-Schiller-Univ. Jena (Germany); A. Tünnermann, Friedrich-Schiller-Univ. Jena (Germany) and Fraunhofer Institute for Applied Optics and Precision Engineering (Germany)

6873 0S **High-average power femtosecond pulse generation from a Yb-doped large-mode-area microstructure fiber laser** [6873-27]
C. Lecaplain, C. Chedot, A. Hideur, Univ. de Rouen (France); B. Ortaç, J. Limpert, Friedrich-Schiller-Univ. Jena (Germany)

6873 0T **Widely tunable femtosecond fiber laser** [6873-28]
A. V. Andrianov, S. V. Muraviev, A. V. Kim, Institute of Applied Physics (Russia); V. F. Khopin, Institute of Chemistry of High Purity Substances (Russia); A. A. Sysoliatin, Fiber Optics Research Ctr. (Russia)

FIBER DAMAGE, UV GENERATION AND LONG PERIOD GRATINGS

6873 0U **Rate equation model of bulk optical damage of silica, and the influence of polishing on surface optical damage of silica** [6873-29]
A. Smith, B. Do, Sandia National Labs. (USA); R. Schuster, D. Collier, Alpine Research Optics (USA)

6873 0V **Analytical solutions for nonlinear waveguide equation under Gaussian mode approximation** [6873-30]
L. Dong, IMRA America, Inc. (USA)

6873 0X **Long-period gratings written in large-mode area photonic crystal fiber** [6873-32]
D. Nodop, Friedrich-Schiller-Univ. Jena (Germany); L. Rindorf, Technical Univ. of Denmark (Denmark); S. Linke, J. Limpert, A. Tünnermann, Friedrich-Schiller-Univ. Jena (Germany)

FIBER FABRICATION AND NEW MATERIALS

6873 0Z **Recent advances in phosphate glass fiber and its application to compact high-power fiber lasers (Invited Paper)** [6873-33]
A. Schülzgen, L. Li, S. Suzuki, V. L. Temyanko, X. Zhu, College of Optical Sciences/The Univ. of Arizona (USA); S. Jiang, C. Spiegelberg, NP Photonics, Inc. (USA); R. M. Rogojan, J. Albert, Carleton Univ. (Canada); N. Peyghambarian, College of Optical Sciences/The Univ. of Arizona (USA)

6873 11 **A new material for high-power laser fibers** [6873-36]
A. Langner, G. Schötz, M. Such, T. Kayser, Heraeus Quarzglas GmbH and Co. KG (Germany); V. Reichel, S. Grimm, J. Kirchhof, Institut für Photonische Technologien e.V. (Germany); V. Krause, G. Rehmann, Laserline GmbH (Germany)

6873 12 **Prospects for laser DEW (Invited Paper)** [6873-37]
D. H. Titterton, Defence Science and Technology Lab. (United Kingdom)

COHERENT AND SPECTRAL COMBINATION

6873 14 **External and common-cavity high spectral density beam combining of high power fiber lasers (Best Student Paper Award)** [6873-39]
O. Andrusyak, The College of Optics and Photonics, Univ. of Central Florida (USA); I. Ciapurin, V. Smirnov, OptiGrate (USA); G. Venus, N. Vorobiev, L. Glebov, The College of Optics and Photonics, Univ. of Central Florida (USA)

6873 15 **Passive coherent phasing of fiber laser arrays** [6873-40]
J. E. Rothenberg, Northrop Grumman Space Technology (USA)

6873 16 **Coherent beam combining of fiber amplifier arrays and application to laser beam propagation through turbulent atmosphere** [6873-41]
P. Bourdon, V. Jolivet, B. Bennai, L. Lombard, G. Canat, E. Pourtal, ONERA (France); Y. Jaouen, GET Telecom Paris (France); O. Vasseur, ONERA (France)

6873 17 **Spectral combining of pulsed fiber lasers: scaling considerations** [6873-42]
O. Schmidt, S. Klingebiel, B. Ortac, F. Röser, F. Brückner, T. Clausnitzer, E.-B. Kley, J. Limpert, Friedrich-Schiller-Univ. Jena (Germany); A. Tünnermann, Friedrich-Schiller-Univ. Jena (Germany) and Fraunhofer Institute for Applied Optics and Precision Engineering (Germany)

SUPERCONTINUUM GENERATION, MODE PROFILING, AND THERMAL MANAGEMENT

6873 18 **Mode profiling of optical fibers at high laser powers** [6873-44]
P. C. Nielsen, D. B. Pedersen, R. B. Simonsen, D. N. Erschens, M. F. Lilbaek, L. Eskildsen, K. Rottwitt, H. N. Hansen, Technical Univ. of Denmark (Denmark)

6873 19 **Optimization of the heat transfer in multi-kW-fiber-lasers** [6873-45]
B. Zintzen, T. Langer, RWTH Aachen (Germany); J. Geiger, D. Hoffmann, ILT Fraunhofer-Institut für Lasertechnik (Germany); P. Loosen, RWTH Aachen (Germany) and ILT Fraunhofer-Institut für Lasertechnik (Germany)

6873 1A **High power 29 W CW supercontinuum source** [6873-46]
B. A. Cumberland, J. C. Travers, S. V. Popov, J. R. Taylor, Imperial College London (United Kingdom)

6873 1B **Highly nonlinear fibers for very wideband supercontinuum generation** [6873-47]
L. Grüner-Nielsen, B. Pálsdóttir, OFS Fitel Denmark ApS (Denmark)

PHOTODARKENING

6873 1C **Photo darkening in ytterbium co-doped silica material** [6873-48]
K. E. Mattsson, S. Nissen Knudsen, Crystal Fibre A/S (Denmark); B. Cadier, T. Robin, iX Fiber (France)

6873 1D **Measurement of high-photodarkening resistance in phosphate fiber doped with 12% Yb_2O_3** [6873-49]
Y. W. Lee, S. Sinha, M. J. F. Digonnet, R. L. Byer, Stanford Univ. (USA); S. Jiang, NP Photonics (USA)

6873 1E **Reduction of photodarkening in Yb/Al-doped fiber lasers** [6873-50]
M. Engholm, Mid-Sweden Univ. (Sweden) and Acreo FiberLab (Sweden); L. Norin, Acreo FiberLab (Sweden)

6873 1F **Radiation damage effects in doped fiber materials** [6873-51]
B. P. Fox, K. Simmons-Potter, J. H. Simmons, The Univ. of Arizona (USA); W. J. Thomes, NASA Goddard Space Flight Ctr. (USA); R. P. Bambha, D. A. V. Kliner, Sandia National Labs. (USA)

6873 1G **Photodarkening in Yb-doped silica fibers: influence of the atmosphere during preform collapsing** [6873-52]
S. Jetschke, S. Unger, A. Schwuchow, M. Leich, V. Reichel, J. Kirchhof, Institute of Photonic Technology (Germany)

CHIRPED PULSE AMPLIFICATION

6873 1I **Large-mode-area Er-doped fiber chirped-pulse amplification system for high-energy sub-picosecond pulses at 1.55 µm** [6873-54]
T. Yilmaz, L. Vaissie, M. Akbulut, D. M. Gaudiosi, L. Collura, T. J. Booth, Raydiance, Inc. (USA); J. C. Jasapara, M. J. Andrejco, A. D. Yablon, C. Headley, D. J. DiGiovanni, OFS Labs. (USA)

6873 1L **Sub 30 fs pulses from 2 MHz repetition rate fiber amplifier pumped optical parametric amplifier** [6873-57]
J. Rothhardt, S. Hädrich, F. Röser, B. Ortac, J. Limpert, Friedrich-Schiller-Univ. Jena (Germany); A. Tünnermann, Friedrich-Schiller-Univ. Jena (Germany) and Fraunhofer Institute for Applied Optics and Precision Engineering (Germany)

6873 1M **Environmentally-stable wave-breaking-free mode-locked Yb-doped all-fiber laser** [6873-58]
B. Ortaç, M. Plötner, Friedrich-Schiller-Univ. Jena (Germany); T. Schreiber, Friedrich-Schiller-Univ. Jena (Germany) and Fraunhofer Institute for Applied Optics and Precision Engineering (Germany); J. Limpert, Friedrich-Schiller-Univ. Jena (Germany); A. Tünnermann, Friedrich-Schiller-Univ. Jena (Germany) and Fraunhofer Institute for Applied Optics and Precision Engineering (Germany)

6873 1N **High repetition rate mode-locked ytterbium fiber laser using dichroic fiber mirrors and photonic bandgap fiber technology** [6873-59]
L. Orsila, R. Herda, O. G. Okhotnikov, Tampere Univ. of Technology (Finland)

POSTER SESSION

6873 1O **Square-root law of turbulence-induced spectral broadening in Raman fiber lasers** [6873-69]
S. A. Babin, D. V. Churkin, A. E. Ismagulov, S. I. Kablukov, E. V. Podivilov, Institute of Automation and Electrometry (Russia)

6873 1P **Characterization of ultra-long Raman fibre lasers** [6873-60]
S. A. Babin, Institute of Automation and Electrometry (Russia); V. Karalekas, Aston Univ. (United Kingdom); E. V. Podivilov, Institute of Automation and Electrometry (Russia); V. K. Mezentsev, P. Harper, Aston Univ. (United Kingdom); J. D. Ania-Castañón, Aston Univ. (United Kingdom) and Instituto de Óptica (Spain); S. K. Turitsyn, Aston Univ. (United Kingdom)

6873 1Q **New mechanism of the mode coupling in multi-core fiber lasers** [6873-61]
A. S. Kurkov, Fiber Optics Research Ctr. (Russia); S. A. Babin, I. A. Lobach, S. I. Kablukov, Institute of Automation and Electrometry (Russia)

6873 1R **SBS mitigation with two-tone amplification: a theoretical model** [6873-66]
T. J. Bronder, T. M. Shay, I. Dajani, A. Gavrielides, C. A. Robin, C. A. Lu, Air Force Research Lab. (USA)

6873 1S **Novel multiple-frequency Q-switched fiber laser by using chirped fiber Bragg grating Fabry-Perot etalon** [6873-71]
X. P. Cheng, P. Shum, C. H. Tse, Nanyang Technological Univ. (Singapore); R. F. Wu, DSO National Labs. (Singapore); W. C. Tan, Nanyang Technological Univ. (Singapore)

6873 1T **High power monolithically integrated all-fiber laser design using single-chip multimode pumps for high reliability operation** [6873-63]
M. Faucher, E. Villeneuve, B. Sevigny, A. Wetter, R. Perreault, Y. K. Lizé, N. Holehouse, ITF Labs. (Canada)

6873 1V **Speckle reduction in multimode fiber with a piezoelectric transducer in radial vibration for fiber laser marking and display applications** [6873-67]
W. Ha, S. Lee, Yonsei Univ. (South Korea); Y. Jung, J. Kim, GIST (South Korea); K. Oh, Yonsei Univ. (South Korea)

6873 1W **Green and UV frequency conversion of a variable pulse repetition frequency photonic crystal fiber system** [6873-77]
E. C. Honea, M. Savage-Leuchs, P. Jones, C. Dilley, Aculight Corp. (USA)

6873 1X **Analytical model for the design of external-cavity passively Q-switched fiber lasers** [6873-75]
J. Y. Huang, H. C. Liang, K. W. Su, Y. F. Chen, National Chiao Tung Univ. (Taiwan)

6873 1Y **Application of optical phase lock loops in coherent beam combining** [6873-80]
W. Liang, N. Satyan, California Institute of Technology (USA); F. Aflatouni, Univ. of Southern California (USA); A. Yariv, California Institute of Technology (USA); A. Kewitsch, G. Rakuljic, Telaris, Inc. (USA); H. Hashemi, Univ. of Southern California (USA)

6873 20 **Performance and reliability of pulsed 1060 nm laser modules** [6873-72]
S. Mohrdiek, J. Troger, T. Pliska, H.-U. Pfeiffer, D. Jaeggi, N. Lichtenstein, Bookham AG (Switzerland)

6873 21 **High-power femtosecond Yb-doped single-polarization photonic crystal fiber laser** [6873-79]
B. Ortaç, Friedrich-Schiller-Univ. Jena (Germany); C. Lecaplain, A. Hideur, Friedrich-Schiller-Univ. Jena (Germany) and Univ. de Rouen (France); J. Limpert, Friedrich-Schiller-Univ. Jena (Germany); A. Tünnermann, Friedrich-Schiller-Univ. Jena (Germany) and Fraunhofer Institute for Applied Optics and Precision Engineering (Germany)

6873 22 **An actively mode-locked fiber laser for sampling in a wide-bandwidth opto-electronic analog-to-digital converter** [6873-65]
J. P. Powers, P. E. Pace, Naval Postgraduate School (USA)

6873 25 **Comparison of photodarkening in ytterbium-doped fibers** [6873-64]
M. Söderlund, J. Montiel, Helsinki Univ. of Technology (Finland); S. Tammela, Corelase Oy (Finland); S. Yliniemi, S. Honkanen, Helsinki Univ. of Technology (Finland)

6873 27 **High power cladding light strippers** [6873-70]
A. Wetter, M. Faucher, B. Sévigny, ITF Labs. (Canada)

Author Index

Conference Committee

Symposium Chairs

Henry Helvajian, The Aerospace Corporation (USA)
Friedrich G. Bachmann, Rofin-Sinar Laser GmbH (Germany)

Symposium Cochairs

Peter R. Herman, University of Toronto (Canada)
Donald J. Harter, IMRA America, Inc. (USA)

Program Track Chair

Gregory J. Quarles, VLOC (USA)

Conference Chairs

Jes Broeng, Crystal Fibre A/S (Denmark)
Clifford Headley, OFS Fitel, LLC (USA)

Conference Cochairs

Denis V. Gapontsev, IPG Photonics Corporation (USA)
Dahv A. V. Kliner, Sandia National Laboratories (USA)

Program Committee

Richard W. Berdine, Air Force Research Laboratory (USA)
Jay W. Dawson, Lawrence Livermore National Laboratory (USA)
Benjamin J. Eggleton, The University of Sydney (Australia)
Almantas Galvanauskas, University of Michigan (USA)
Anderson S. L. Gomes, University Federal de Pernambuco (Brazil)
Donald J. Harter, IMRA America, Inc. (USA)
Johan Nilsson, University of Southampton (United Kingdom)
Kyunghwan Oh, Yonsei University (South Korea)
Jasbinder S. Sanghera, Naval Research Laboratory (USA)
Kanishka Tankala, Nufern (USA)
Andreas Tünnermann, Fraunhofer Institut für Angewandte Optik und Feinmechanik (Germany)
Ken-ichi Ueda, The University of Electro-Communications (Japan)
Robert G. Waarts, Raydiance Inc. (USA)
Benjamin G. Ward, U.S. Air Force Academy (USA)
Yoann Zaouter, Bordeaux University (France)
Luis A. Zenteno, Corning Inc. (USA)

Session Chairs

1 Fiber Laser Market
Denis V. Gapontsev, IPG Photonics Corporation (USA)

2 Fiber Designs
Kanishka Tankala, Nufern (USA)

3 Pulsed Sources
Jay W. Dawson, Lawrence Livermore National Laboratory (USA)

4 Bulk-Fiber Hybrid Lasers: Joint Session with Conference 6871
Dahv A. V. Kliner, Lawrence Livermore National Laboratory (USA)
Norman Hodgson, Coherent, Inc. (USA)

5 IR-Sources
Dahv A. V. Kliner, Lawrence Livermore National Laboratory (USA)

6 Narrowlinewidth Sources and SBS Suppresion
Luis A. Zenteno, Corning, Inc. (USA)

7 Femtosecond Lasers
Donald J. Harter, IMRA America, Inc. (USA)

8 Fiber Damage, UV Generation and Long Period Gratings
Benjamin G. Ward, U.S. Air Force Academy (USA)

9 Fiber Fabrication and New Materials
Kanishka Tankala, Nufern (USA)

10 Coherent and Spectral Combination
Richard W. Berdine, Air Force Research Laboratory (USA)

12 Supercontinuum Generation, Mode Profiling, and Thermal Management
Andreas Tünnermann, Fraunhofer Institut für Angewandte Optik und Feinmechanik (Germany)

13 Photodarkening
Johan Nilsson, University of Southampton (United Kingdom)

14 Chirped Pulse Amplification
Yoann Zaouter, Bordeaux Université (France)

High power fused pump/signal combiner for reverse pumping of active double clad fibers

Ole Lumholt, Søren Agger, Thomas T. Alkeskjold, Kate B. Bing, Mark Denninger and Thomas Nikolajsen
Crystal Fibre A/S, Blokken 84, DK-3460 Birkerød, Denmark

ABSTRACT

We present a new type of combiner based on a fused pump/signal fiber bundle. We obtain a record high signal-to-pump isolation of more than 46dB from a device optimized for high power counter directional pumping of Ytterbium-doped large mode area airclad fibers. The compact device combines more than 100W of light from 14 pcs. of 105µm NA=0.15 fibers into the pump cladding of an airclad fiber with a coupling efficiency of 90%. The signal light is delivered through the center of the combiner ensuring the exceptional isolation. The high level of isolation, measured for a 60W amplifier configuration, is essential to ensure the reliability of the pump diodes in a high power pulsed system. The combiner is compatible with PM and non-PM systems and we demonstrate both a CW and a pulsed configuration.

Keywords: Fiber optics components, double-clad fibers, high-power pulsed fiber lasers

1. INTRODUCTION

Within the last few years, the Ytterbium-doped double-clad fiber amplifiers have developed from niche applications lasers into the high-power laser industry for material processing [1]. Fibre lasers offer a unique combination of high beam quality and high output powers, but handling of high peak powers in the fiber core limits performance by the onset of optical nonlinearities or by optical damage.

Expanding the core size of the fiber reduces the power density, thus reducing nonlinear effects and increasing damage threshold levels. But to take full advantage of large mode field areas, it is essential to use a counter propagating pump configuration. Such a configuration has two important impacts. It offsets the nonlinearities due to a shorter effective length compared to the forward pumped configuration. Additionally it increases fiber lifetime, as it reduces effects of photo darkening due to a lower local inversion as compared to a forward pump scheme. However, the major concern for a high output power, backward pumped configuration is the pump laser damage that is caused by signal power leaking into the pump branches.

We demonstrate a new type of pump/signal combiner for counter directional pumping of large mode area (LMA) airclad fibers. The combiner is designed to give unique signal to pump isolation. We utilize the high numerical aperture (NA) of the airclad, to make a NA division multiplexing in which signal and pumps are completely separated in space. This amplifier module offers the full benefits of the LMA fiber amplifier that is high average output powers together with low nonlinearities. It thus finds applications in high power CW single-frequency or high peak power / high energy pulse amplification.

2. BASIC PRINCIPLE OF THE COMBINER

The basic principle of the component is to utilize the high NA of Photonic Crystal Fiber (PCF) airclads, to couple low NA light from off-axis co-directional oriented standard fibers via a reflective element. See Fig. 1. The large NA difference, between a PCF with NA=0.6 and a pump fiber with NA=0.15, allows for the launch of pump power only through the high angled part of the PCF acceptance cone, leaving the low angled part isolated from the pump path. See Fig. 2. The amplified signal leaves the PCF in free space through the latter and is fed through a pinhole in the centre of the reflective element. The complete separation of signal and pump at the reflective element ensures a very high isolation between the amplified signal and the pumps. In the configuration reported here, the PCF has a 40µm polarizing core,

200µm inner and 450µm outer cladding. The circular symmetrical geometry allows for the stacking of 14 standard 105µm core, 125µm cladding diameter multimode pump fibers around the PCF. All fibers are fused together to form a fused fiber bundle to ensure stability and enable high power handling. Fig. 3 shows an example of a fused fiber bundle around a PCF with stress elements.

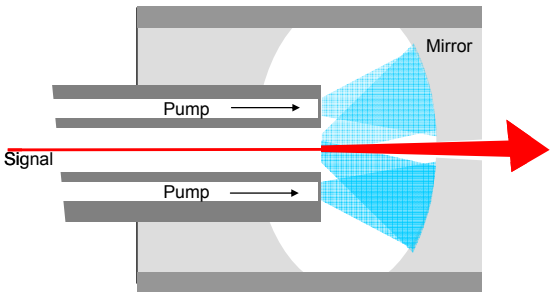

Fig. 1. Curved mirror setup

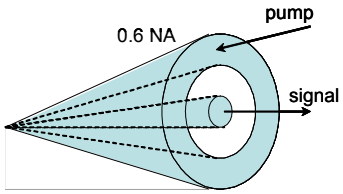

Fig. 2. PCF acceptance cone

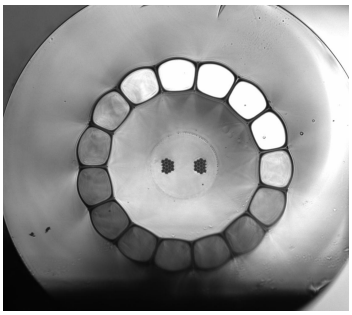

Fig. 3. Fused fiber bundle

Fabrication of the fused bundle requires a careful stacking process of pump fibers to locate them symmetrically around the PCF in a sleeving tube. This whole assembly is fused on a glass processing unit to form a fully fused glass component. Pressurizing the PCF during the fusing ensures that airclad fiber characteristics are preserved during processing. End sealing of the cleaved fused fiber bundle allows for angle polish of the sealed component. The mirror used is made of low oxygen copper as it has 98% reflectivity for pump wavelengths of interest and in addition a high thermal conductivity. A 0.2mm precisely located feed through hole ensures good tolerances for the amplified signal (NA=0.04) with no overlap to the pump reflecting region. The mirror is mechanically fixed to the bundle house which again is fixed to the fused bundle to form a fully packaged device.

3. POWER MEASUREMENTS

The pump coupling efficiency is measured on a packaged device having a passive, core-free centre fiber. By launching with power from 14 standard single-emitter diodes, we obtain 100W of coupled pump power with 90% coupling efficiency. This is close to the theoretical max, as we have to account for two times 4% Fresnel reflection at the free ends of the PCF as well as a 2% loss from the mirror surface. We examined the time stability during a 2 hours test period. As shown in Fig. 5, no degradation occurs except for the initial 10 min warm up period of the single emitter diodes.

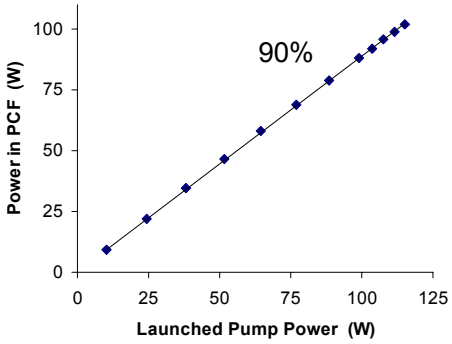

Fig. 4. Coupled and guided pump power in the PCF vs. launched power on mirror

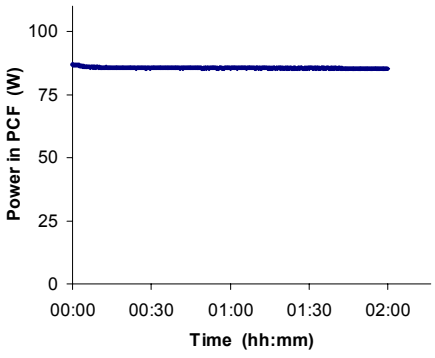

Fig. 5. Coupled pump power, time dependence.

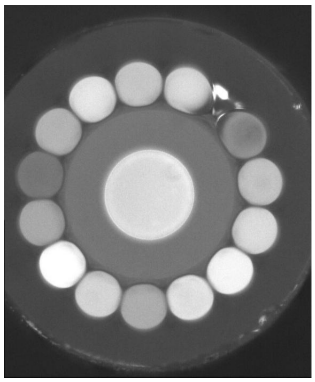

Fig. 6. Illuminated bundle

We also tested a combiner with the 40µm core, active fiber in a laser configuration by mounting a high reflective mirror at the free fiber end and using the back reflection from the facet of the fused fiber bundle in the other end. We obtained 67% slope efficiency at 60W of output power from this laser configuration.

As mentioned, a high isolation between amplified signal and pump diodes is a critical parameter for pump combiners in counter propagating configurations. Consider a realistic damage level for a pump diode to 0.2µJ pulse energy. A 1mJ pulse delivery system in a backward pump configuration then requires at least 37dB signal to pump isolation. Measurements of traditional tapered fiber bundle combiners give isolation in the vicinity of 20dB. In our experiment the isolation of reflected signal light into a pump fiber was measured to be >46dB at high power levels, see Fig. 8, corresponding to 1.5mW at 60W output. The 1.5mW of detected light is mainly due to light leaking out of the core of the active fiber and into the cladding. The level of this light depend very much on the ability to launch light into the amplifier on the input side and therefore is a number which can be further optimized if needed. As the ratio between amplified core light and the cladding light increases for increasing power level, the isolation is seen to increase for increased signal output power.

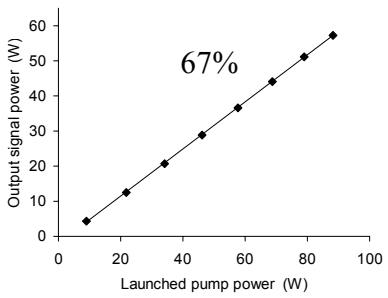

Fig. 7. Laser output power

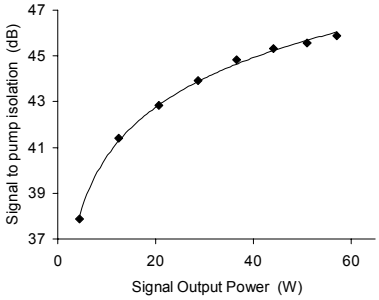

Fig. 8. Signal to pump isolation

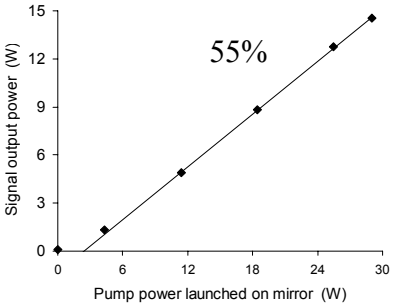

Fig. 9. Amplified output power

Finally, we tested the combiner in an amplifier configuration with a polarized 1064nm seed coupled to the PCF input end by bulk optics. The amplified signal core light was detected through a pin-hole at the output end of the combiner feed-through tunnel to eliminate cladding light. We obtained 15W of signal output power with 55% slope efficiency for CW operation. We measured the polarization extinction ratio to well above 20dB. In pulsed operation using an amplified gain-switched seed laser delivering 10ns pulses at 250kHz repetition rate, we obtained 5kW peak power, limited alone by the seed source available. The fiber itself has shown capable of handling almost 1MW peak power [2].

4. CONCLUSION

A new type of fused pump/signal combiners with high signal to pump isolation is presented. A unique signal to pump isolation of 46dB ensures sufficient isolation for mJ pulse operation of Ytterbium doped airclad fibers in backward pump configurations without damaging the pump diodes. The device based on a fused fiber bundle of 14 standard multimode fibers and a double clad Yb-doped 200/41 airclad fiber is shown capable of handling in excess of 100W of pump power. We measured 60W of output power from the component in a laser configuration with 67% slope efficiency.

REFERENCES

1 J. Limpert, A. Liem, M. Reich, T. Schreiber, S. Nolte, H. Zellmer, A. Tunnermann, J. Broeng, A. Petersson and C. Jacobsen “Low-nonlinearity single-transverse-mode ytterbium-doped photonic crystal fiber amplifier”, Optical Express, Vol. 12, No. 7, April 5 (2004), pp 1313-1319.

2 C.D. Brooks and F.D. Teodoro “High peak power operation and harmonic generation of a single-polarization, Yb-doped photonic crystal fiber amplifier”, Optics Communications, Vol. 280, No. 2, Dec. 15 (2007), pp 424 – 430.

Single-polarization single-transverse-mode rod-type photonic crystal fiber with mode-field-area of 2300 μm^2

O. Schmidt, J. Rothhardt, T. Eidam, F. Röser, J. Limpert, A. Tünnermann
Friedrich-Schiller-University Jena, Institute of Applied Physics, Max-Wien-Platz 1, D-07743 Jena, Germany

K.P. Hansen, C. Jakobsen, J. Broeng
Crystal Fibre A/S, Blokken 84, DK-3460 Birkeroed, Denmark

Abstract. : We report on an ytterbium-doped single-transverse-mode rod-type photonic crystal fiber that combines the advantages of low nonlinearity and intrinsic polarization stability. The mode-field-area of the fundamental mode is as large as 2300 μm^2. An output power of up to 163 W with a degree of polarization better than 85% has been extracted from a simple fiber laser setup without any additional polarizing element within the cavity than the fiber itself. The beam quality has been characterized by a M^2 value of 1.2. The single-polarization window ranges from 1030 to 1080 nm, hence possesses an excellent overlap with the gain profile of ytterbium-doped silica fibers. To the best of our knowledge this fiber design has the largest mode-field-diameter ever reported for polarizing or even polarization maintaining rare-earth-doped double-clad fibers.

Introduction

The performance of rare-earth-doped fiber laser systems is primarily limited by nonlinear effects. Hence, over the recent years every endeavor has been made to develop fiber designs with reduced nonlinearity. Fiber designs with core diameter up to 100 μm have been reported, which are able to support stable fundamental mode propagation [1]. However, a degradation of the degree of polarization (DOP) is typically observed when using non-polarization maintaining fibers. To overcome this problem and especially to simplify the laser setup in terms of polarization control there is a great interest in combining large mode area microstructured fibers and polarization maintaining elements. Several approaches have been reported to achieve this, such as the well-known technique of stress-applying parts (SAP) inside a step-index large-mode-area low-numerical aperture fiber [2] or a SAP in combination with the photonic crystal cladding in microstructured fibers. The latter technique gives even the possibility to split (due to introduced birefringence) the two polarization states of the weakly guided fundamental mode in that way, that the effective index of one polarization is below the cladding index, thus, resulting in a single polarization large mode area fiber. An Ytterbium-doped single-polarization fiber with mode-field-areas of about 700 μm² has been reported recently [3].

In this contribution we report on continuous-wave fiber laser comprising a 70 μm core single-polarization, single-transverse mode photonic crystal fiber. The fiber laser shows a high DOP without any additional polarization controlling intracavity element up to pump-power limited output powers as high as 163 W. The comparison with a standard (non-polarizing) fiber with similar dimension shows the advantages and the potential of the fiber including SAPs in terms of polarization control.

Experimental setup and results

A simple continuous-wave fiber laser is setup to evaluate the polarizing properties of the large-mode-area Yb-doped PCF. The active fiber (Crystal Fibre, DC-200/70-PM-Yb-ROD) possesses a 200 μm inner cladding with a numerical aperture of 0.6, in which the 976 nm pump light is launched. 19 holes of the photonic cladding are missing to form the 70 μm diameter core. The structure has a small signal pump light absorption at 976 nm of ~30 dB/m. A cross section of the fiber is shown in Fig. 1, clearly indicating the boron-doped SAPs.

The laser cavity is built up by a high reflective mirror and the 4% Fresnel reflection at the perpendicularly cleaved output facet of the fiber. At maximum available pump power an output power of 163 W is reached with a slope efficiency of ~75 % and an emission wavelength around 1035 nm (no wavelength selection introduced). Figure 2 shows the DOP (DOP = P_{max}-P_{min} / P_{max}+P_{min}) as a function of the launched pump power. The results obtained for the fiber with SAPs are compared to a very similar fiber possessing an 80 μm active core but without SAPs. An identical length of fiber is used in the same fiber laser cavity. As shown, the DOP of the large-mode-area single-polarization PCF maintains the linear polarization state (DOP > 85 %) with increasing power. In contrast, the non-PZ fiber shows more or less uncontrolled as wells as temporally unstable polarization evolution.

The characterization of the emission reveals a slightly asymmetric mode possessing a mode field diameter of 50 and 57 µm, respectively. The corresponding mode-field-area is as large as 2300 µm^2. The beam quality is measured to be better than 1.2 for the complete power range discussed above.

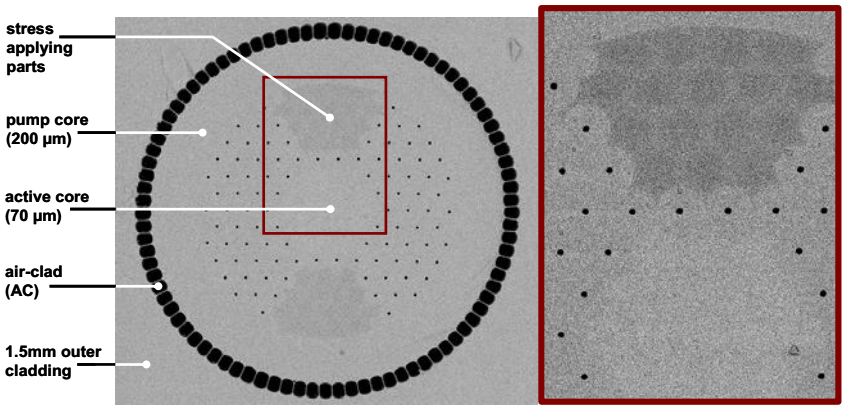

Fig. 1. Cross-section of the polarizing large-mode-area PCF with a zoom on the embedded stress applying parts.

A tunable diode laser is used to characterize the single polarization window of the large-mode-area PZ-PCF. The measurement revealed a high confinement loss for both polarization states below 1030 nm, low-loss propagation for the slow axis and still high losses for the fast axis mode for wavelengths ranging from 1035 to 1080 nm. Above 1080 nm both polarization states are confined and the fiber structure works in a polarization maintaining manner. Figure 3 shows near field intensity distributions for the slow and fast axis which are characteristic for the three wavelength ranges. It should be mentioned that the transitions between these regimes are rather smooth than discrete.

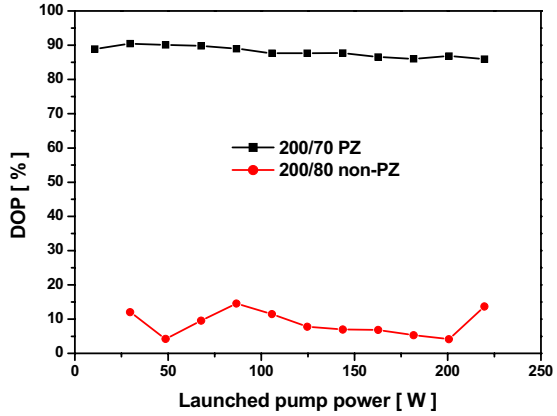

Fig. 2.: DOP vs. launched pump power for polarizing and non-polarizing rod-type fibers.

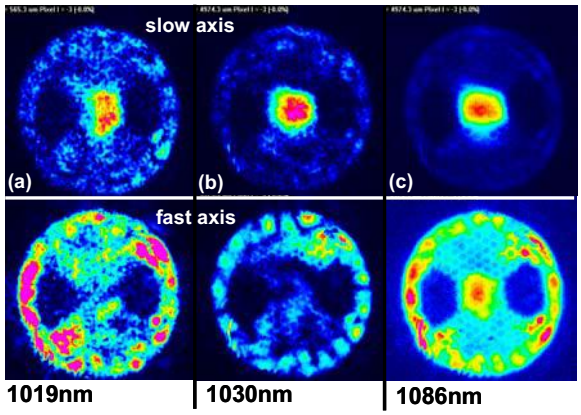

Fig. 3.: Near field intensity distributions for the slow and fast axis at three different wavelengths.

In conclusion, we have reported on a large-mode-area (2300 µm^2) single-transverse mode single-polarization ytterbium-doped photonic crystal fiber. To our knowledge this is the largest polarizing or even polarization maintaining fiber design ever demonstrated. The polarizing properties have been proven in a high power fiber laser setup without any additional polarization control. The single-polarization window of the presented fiber design ranges from 1030 to 1080 nm, hence possessing a good overlap with the Yb gain profile, making this fiber highly interesting for high peak power and high energy fiber laser and amplifier configurations.

References

1. C. D. Brooks, F. Di Teodoro "Multimegawatt peak-power, single-transverse-mode operation of a 100 µm core diameter, Yb-doped rodlike photonic crystal fiber amplifier," Appl. Phys. Lett. **89**, 111119 (2006).
2. C.-H. Liu, A. Galvanauskas, V. Khitrov, B. Samson, U. Manyam, K. Tankala, D. Machewirth, S. Heinemann, "High-power single-polarization and single-transverse-mode fiber laser with an all-fiber cavity and fiber-grating stabilized spectrum," Opt. Lett. **31**, 17-19 (2006).
3. T. Schreiber, F. Röser, O. Schmidt, J. Limpert, R. Iliew, F. Lederer, A. Petersson, C. Jacobsen, K. Hansen, J. Broeng, A. Tünnermann, "Stress-induced single-polarization single-transverse mode photonic crystal fiber with low nonlinearity," Opt. Express **13**, 7621-7630 (2005).

Spatially and spectrally resolved imaging of higher-order-modes in large-mode-area fibers

J.W. Nicholson and A.D. Yablon
OFS Laboratories, 19 Schoolhouse Road, Suite 105, Somerset NJ, 08873
Phone: (732) 748-7489; email: jwn@ofsoptics.com

Abstract: Higher-order modes propagating in large-mode-area fibers are characterized using spatially-and spectrally resolved modal imaging. The measurements provide the fraction of power contained in multiple higher-order-modes, and allow for mode identification, and quantify beam pointing instabilities.

Large-mode-area (LMA) fibers have enabled recent advances in high-power fiber lasers and amplifiers. However, many applications of fiber lasers depend on the quality of the beam profile. While single-mode fibers (SMF) are known for their excellent beam quality, as the effective area (A_{eff}) is pushed larger to enable high power operation and mitigate nonlinearities, the fiber begins to support increasing numbers of higher-order-modes (HOMs) which can degrade the output beam quality.

A typical measure of the quality of an optical beam is the M^2 parameter [1]. However, even when the amount of power contained in a higher-order-mode becomes very large, it is still possible to achieve a low value of M^2 [2]. Even worse, changing the relative phase of the modes propagating in the fiber can lead to pointing instabilities in the far field. Consequently, new techniques are required to characterize optical beams from LMA fibers capable of supporting multiple HOMs.

Measurements capable of quantifying the partially coherent, transverse mode content from bulk-optic laser resonators only require measuring the transverse beam intensity profiles [3,4]. The situation where the modes are coherent requires more information, however. In this paper we introduce a new measurement technique capable of simultaneously imaging multiple, coherent, higher-order modes propagating in an LMA fiber. Not only can the types of modes and their relative power levels be quantified, but the measured data also provides the level of Poynting vector instability in the beam caused by fluctuating phases between the modes. We refer to this technique as ***S***patially and ***S***pectrally resolved imaging of fiber modal content, or more simply as S^2 imaging.

The S^2 imaging setup for measuring the higher-order-mode content of an LMA fiber is shown in Figure 1a. Light from a broadband source is launched into the LMA test fiber. At the exit of the LMA fiber the beam is re-imaged with magnification onto the cleaved end of a single mode fiber which is coupled into an optical spectrum analyzer (OSA). A polarizer ensures that the polarization state of the modes is aligned on the SMF end-face.

The probe fiber, single-moded at the measurement wavelength, is placed on automated translation stages to move the fiber end in x and y directions perpendicular to the beam propagation direction. The SMF fiber is rastered in *x* and *y*, and at each *(x,y)* point the optical spectrum is measured. A typical optical spectrum measured at an arbitrary *(x,y)* point is plotted in Figure 1b. If two different modes overlap spatially in the near-field at that *(x,y)* point, they will have a spectral interference pattern due to group delay differences between the modes in the fiber under test. It is this spatially and modally dependent spectral interference pattern that is used to simultaneously image multiple HOMs propagating in the LMA fiber and also quantify their relative power levels.

The LMA test fiber for this experiment had a 20 μm mode-field diameter (MFD). The single mode output fiber of an Yb ASE source was spliced with a mode-matching splice to a 20m length of LMA fiber. Figure 2a shows the beam profile obtained by integrating the measured spectrum at each *(x,y)* point. A sum of the Fourier transforms of all the measured optical spectra from each spatial point is shown in Fig. 2b. There are clearly several different beat frequencies visible, corresponding to interference between the primary LP_{01} mode and different higher order modes. Because the LP_{01} mode is the dominant mode, interference between two different HOMs is considered negligible.

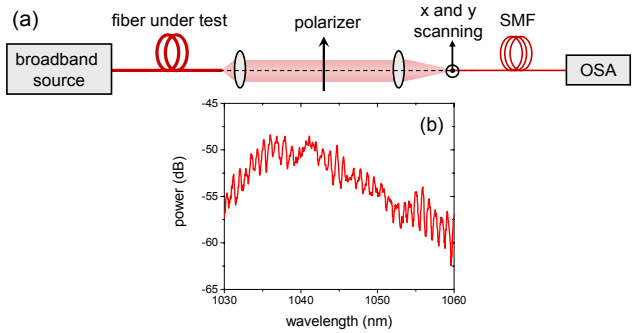

Fig. 1: (a) Setup for characterizing the higher order mode content in LMA fibers using spatially resolved modal interference. (b) Optical spectra measured at an arbitrary *(x,y)* point showing interference between fiber modes.

In order to calculate the relative power levels of the modes using the Fourier transform of the measured optical spectra, we assume two modes with spatially and frequency dependent amplitudes, $A_1(x,y,\omega)$ and $A_2(x,y,\omega)$, related by a constant $\alpha(x,y)$, such that

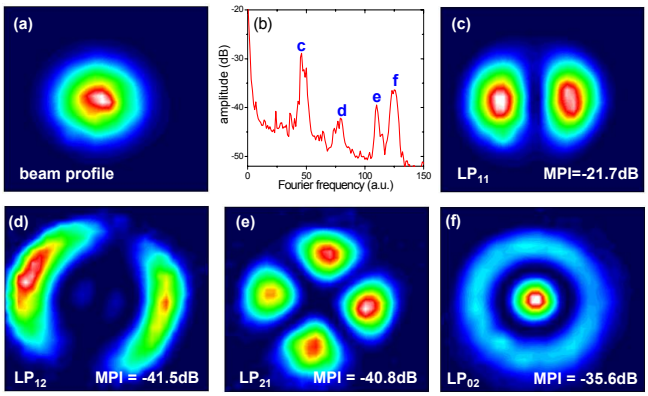

Fig. 2: (a) Beam profile from the LMA fiber. (b) Fourier transform of the optical spectra. (c)–(f) Images of higher order modes corresponding to the Fourier peaks in (b) and their MPI levels with respect to the LP_{01} mode.

$A_2(x,y,\omega) = \alpha(x,y)\, A_1(x,y,\omega)$. The multi-path-interference (MPI), or the ratio of powers P_1 and P_2 in the modes, is obtained by integrating over the mode intensities,

$$MPI = 10\log\left[\frac{P_2}{P_1}\right] = 10\log\left[\frac{\iint \alpha^2(x,y)\, I_1(x,y)\, dx\, dy}{\iint I_1(x,y)\, dx\, dy}\right].$$

The spatially dependent Fourier transform of the optical spectrum is then used to calculate $\alpha(x,y)$. At a given (x,y) point, the ratio $f(x,y)$ is defined as the amplitude of the Fourier transform of the spectral intensity at a Fourier frequency divided by the amplitude at Fourier frequency zero. If it is assumed that $A_1(x,y,\omega)$ and $A_2(x,y,\omega)$ have the same frequency dependence and that the phase difference between the two modes is linear in frequency then it can be shown that $\alpha(x,y)$ is simply related to $f(x,y)$ by

$$\alpha(x,y) = \left\{1 - \sqrt{1 - 4f^2(x,y)}\right\} \Big/ \{2f(x,y)\}.$$

Figures 2c – 2f show the result of this calculation applied to the various peaks observed in the Fourier transform of the optical spectra in Fig. 2b. A variety of higher order modes were observed, clearly identifiable by their spatial patterns as LP_{11}, LP_{12}, LP_{21}, and LP_{02}. The strongest mode, the LP_{11}, was 21.7 dB weaker than the LP_{01}.

An alternative way of analyzing the S^2 data set is to appreciate that a unique beam profile is being measured at each wavelength, and because the different modes in the fiber have different group delays, varying the measurement wavelength effectively samples possible relative phases between the modes. Consequently, beam profiles at different wavelengths correspond to different states of constructive and destructive interference between the modes. This changing interference pattern then leads to pointing instabilities in the beam as was discussed in [2]. Analyzing the data in this manner allows the MPI levels of the higher order modes calculated in the spectrum's Fourier domain to be correlated with the level of Poynting vector instability in the spatial domain.

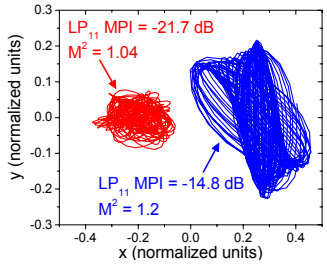

Fig. 3: Center-of-mass movement normalized to the beam diameter for two LMA fibers. Red: fiber shown in Fig. 2. Blue: second fiber with -14.8 dB LP_{11} MPI.

Figure 3 shows the measured motion of the center-of-mass (COM) of the beam versus wavelength for two different LMA fibers with 20 μm MFD. In red is the movement of the COM for the fiber whose modes are analyzed in Fig. 2. The beam movement was normalized to the beam diameter (twice the square root of the beam's second moment). The COM moved by as much as 15% of the beam diameter. Even though the beam COM showed substantial movement, the measured M^2 was as low as 1.04. A second 20 μm MFD fiber was also measured with the S^2 imaging setup, and was found to have -14.8 dB MPI in the LP_{11} mode, with the COM moving by as much as 40% of the beam diameter (Fig. 3, blue curve). The measured M^2 of this fiber still had a value of 1.2. Although the movement of the COM in Figure 3 is observed versus wavelength, it should be emphasized that any perturbation to the fiber that causes a change in the relative phases of the modes propagating in the fiber will cause a similar movement in the beam. Such large movements of the COM, for beams with what would traditionally be considered very good M^2 values, could have significant impact on experiments that depend on beam pointing stability.

In summary, S^2 imaging is a new technique which provides a wealth of detailed information on modal content unavailable from a simple M^2 measurement. The sensitive measurement is capable of quantifying the number, type, and relative power levels of higher-order-modes simultaneously propagating in a large-mode-area fiber and also provides information about movement and distortion of the beam due to fluctuating phases between the modes. No prior knowledge of the dispersive properties of the fiber is required to identify the modes. This technique can be usefully applied to measurements such as LMA component characterization, bend loss measurement of high-order-modes, differential gain measurements of modes in large-mode-amplifiers, and LMA fiber splice optimization.

References

[1] A. E. Siegman, Proc. SPIE 1868, 2 (1993)
[2] S. Wielandy, Opt. Express 15, 15402-15409 (2007)
[3] F. Gori, M. Santarsiero, R. Borghi, and G. Guattari, Opt. Lett, 23, 989 (1998).
[4] C. Rydberg and J. Bengtsson, Opt. Express 15 13613 (2007).

High power nanosecond pulse amplification at 2-microns in thulium-doped fiber pumped at 795nm

Daniel Creeden*[a], Peter A. Budni[b], Peter A. Ketteridge[a]
[a]BAE Systems, Advanced Systems and Technology, PO Box 868, Nashua, NH 03061-0868

ABSTRACT

Rare earth-doped fibers allow for efficient pulse amplification at a variety of wavelengths. Eyesafe pulses are of interest for numerous applications, and traditionally, this has been achieved with Er- or Er:Yb-doped fibers operating at 1.5-microns. Thulium-doped fibers allow for eyesafe pulse amplification in the 2-micron spectral region. We have demonstrated high power nanosecond pulse amplification in a Tm-doped fiber pumped at 795nm. Under constant pump power, we have generated more than 30W of average output power at 100kHz and >18W of average power at 50kHz. With our fiber setup, we are able to produce high output power, pulse energy, and peak-power pulses over a range of repetition rates.

Keywords: fiber amplifiers, TDFA, pulse amplification

1. INTRODUCTION

Fiber lasers and amplifiers are attractive for high power applications, providing high efficiency and good beam quality. Thulium-doped fibers operated CW have recently produced high average powers with high efficiency by pumping at 795nm [1]. The thulium ions allow for very high efficiency operation as a result of the 2-for-1 cross-relaxation of the $^3F_4 \rightarrow {}^3H_4$ transition. In this paper, we discuss the power scaling of our oscillator-amplifier Tm-doped fiber system based on this 795nm pumped Tm-doped large-mode-area (LMA) fiber technology [2]. To our knowledge, this work represents the highest average output power achieved from a pulsed, high repetition rate Tm-doped fiber system.

2. SYSTEM AND RESULTS

The system used in these experiments consists of a seed source, which generates 2-micron pulses, followed by a series of Tm-doped fiber amplifiers (TDFA). The seed is a gain-switched Tm-doped fiber laser, built by Stocker Yale, capable of generating nanosecond pulses at variable repetition rates (50-100kHz) [3]. The first amplifier is a 25μm core, 250μm cladding LMA fiber pumped by a single 25W 795nm diode. The second amplifier is a 25μm core, 400μm cladding LMA Tm-doped fiber pumped at 795nm. A schematic of the system is shown in Fig. 1.

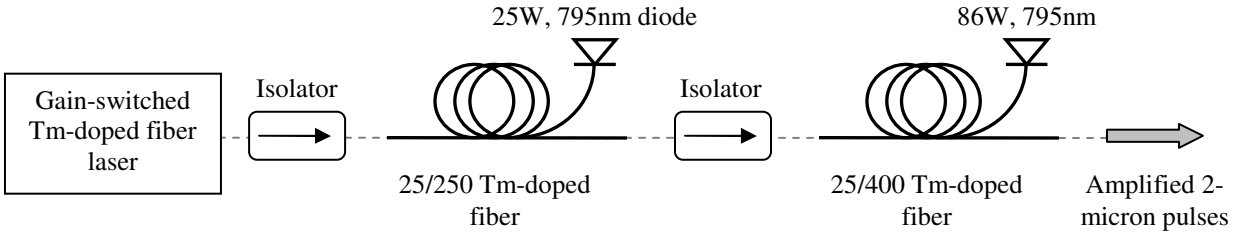

Fig. 1. Tm-doped fiber oscillator and amplifier schematic.

The oscillator produces pulses 15-20ns pulses, depending on the repetition rate. At 50kHz, 15ns pulses are generated; at 100kHz, 20ns pulses are generated.

*daniel.creeden@baesystems.com; phone 1 603 885-4313; fax 1 603 885-0207

This change in pulse width is a result of the reduced gain in the oscillator cavity due to the higher repetition rate. The first amplifier is used as a preamplifier and produces 18dB of gain to the input signal. The second amplifier is a power amplifier, producing 14dB of gain. In between each stage is a free-space optical isolator to prevent feedback from affecting the amplifiers or the oscillator. The power amplifier performance and output beam quality measurements are shown in Fig. 2.

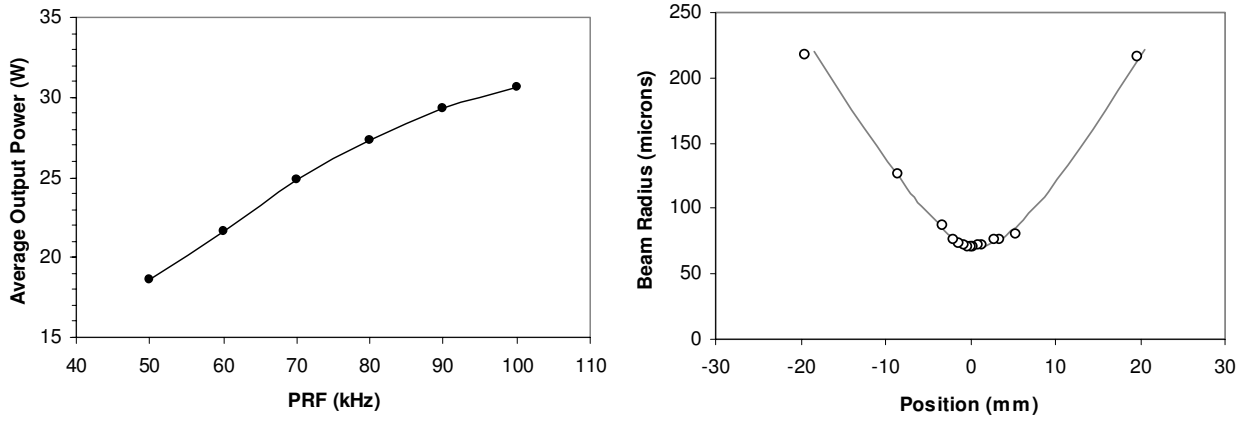

(a) (b)

Fig. 2. (a) Average output power versus PRF from power amplifier under constant pump power of 86W; (b) beam quality measurement from the fiber system - data points represent actual measured data while the dotted line represents a Gaussian fit.

At 50kHz PRF, more than 370uJ is produced at a pulse width of 15ns, resulting in >28kW of peak-power. At 100kHz, 30.6W of average output power is generated (306μJ pulse energy, 15kW peak-power) with a 35% optical efficiency.

In addition, the system produces a near-diffraction-limited beam. The beam quality was measured by focusing the output from the last fiber amplifier through a lens and measuring the spot size of the beam on a pyroelectric array as a function of position through the Rayleigh range. A Gaussian fit to the measured data shows that the output beam is 1.2 times diffraction limited. In this experimentation, we did not observe any amplified spontaneous emission (ASE) or nonlinear effects in the fiber.

3. CONCLUSION

Using the advances in LMA fiber technology, we have demonstrated efficient, high power, eyesafe pulse amplification at 2-microns in a Tm-doped silica fiber. By pumping at 795nm we take advantage of the 2-for-1 cross-relaxation of the thulium ions, resulting in efficient amplification.

These results show the feasibility for Tm-doped fiber to be used as a high power, short-pulse, diffraction-limited eyesafe fiber source. Future work will focus on improving efficiency and scaling output power and pulse energy while maintaining beam quality.

REFERENCES

[1] M. O'Connor, G. Frith, A. Carter, D. P. Machewirth, B. Samson, and K. Tankala, "Highly Efficient, Monolithic Fiber Amplifiers Operating at 2 μm," in *Proceedings of the Solid-State and Diode Laser Technology Review* (2007).

[2] D. Creeden et al., "Mid-Infrared ZGP Parametric Oscillator Directly Pumped by a Pulsed 2μm Tm-doped Fiber Laser," Opt. Lett. (to be published).

[3] M. Jiang and P. Tayebati, "Stable 10 ns, kilowatt peak-power pulse generation from a gain-switched Tm-doped fiber laser," Opt. Lett. **32**, 1797-1799 (2007).

Millijoule Pulse Energy High Repetition Rate Femtosecond Fiber CPA System: Results, SHG and Scaling potential

F. Röser, J. Rothhardt, T. Eidam, O. Schmidt, D.N. Schimpf, J. Limpert, and A. Tünnermann
Friedrich-Schiller-Universität Jena, Institut für Angewandte Physik, Albert-Einstein-Str. 15, D-07745 Jena, Germany
e-mail address: fabian. roeser@.uni-jena.de

Abstract. We report on an ytterbium-doped fiber CPA system delivering millijoule level pulse energy at repetition rates above 100 kHz corresponding to an average power of more than 100 W. The compressed pulses are 800 fs. At 200 kHz repetition rate the pulses were frequency-doubled to 41 W average power and 205 µJ of pulse energy in the green. To show the average power scaling potential of this particular fiber a cw laser experiment was conducted resulting in 710 W of pump-power limited output.

Fiber lasers and amplifiers have the reputation to be immune against thermo-optical distortions due to the fiber geometry itself and the diffraction-less confined propagation of the laser radiation. Hence, they are considered as an average power scalable solid-state laser concept. However, the extraction of ultra-short laser pulses possessing high peak powers is significantly more challenging than in bulk laser systems due to the high intensities in the fiber core sustained over considerable interaction length, which evoke nonlinear pulse distortions, mainly by self-phase modulation (SPM). Fiber CPA systems with reduced nonlinearity applying ytterbium-doped large-mode-area step-index fibers as main amplifier with pulse energies of a few 100 µJ have been presented years ago [1]. Those systems operated at low repetition rates, abandoning the advantages of fiber lasers in terms of average power and were pushed to surprisingly high B-integrals. Here we report on a two-stage fiber CPA system comprising an 80 µm ytterbium-doped core photonic crystal fiber as main amplifier delivering compressed pulse energies up to 1 mJ and average powers up to 100 W at repetition rates up to 200 kHz. The setup consists of a passively mode-locked Yb:KGW oscillator, a dielectric grating stretcher-compressor unit, an acousto-optical modulator as pulse selector and two ytterbium-doped photonic crystal fibers both used in single-pass configuration as amplification stages.

The long-cavity Yb:KGW oscillator delivers transform-limited 400 fs pulses at a repetition rate of 9.7 MHz and an average power of 1.6 W at 1030 nm center wavelength. The stretcher-compressor-unit employs two 1740 lines/mm dielectric diffraction gratings and stretches the 3.3 nm bandwidth pulses to 2 ns. A quartz based acousto-optical modulator is used to reduce the pulse repetition rate and possesses diffraction efficiency as high as 75 %. The pre-amplifier comprises a 1.2 m long 40 µm core single-polarization air-clad photonic crystal fiber pumped by a fiber coupled diode laser emitting at 976 nm. This stage is capable of delivering a single-pass gain as high as 35 dB and average powers up to 6 W. However, we have operated the preamplifier just up to a few µJ of pulse energy to avoid excessive accumulation of nonlinear phase in this stage. The main amplifier is constructed using a low-nonlinearity air-cladding photonic crystal rod-type fiber similar to the fiber presented in [2]. The inner cladding has a diameter of 200 µm (NA = 0.58), the active core is as large as 80 µm. This structure possesses a small signal pump light absorption at 976 nm of 30 dB/m. The fiber has no polymer coating and is embedded in a water cooled aluminum

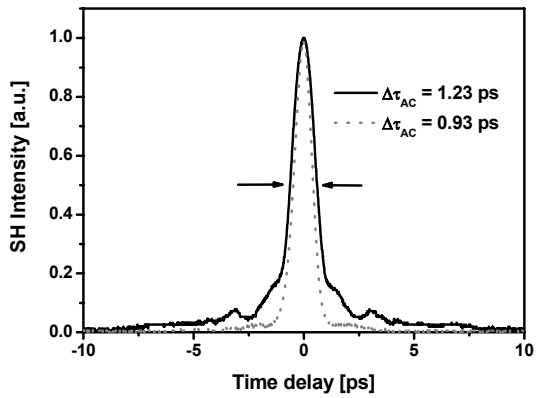

Fig.1. Measured autocorrelation traces of the compressed pulses; dotted: low pulse energy, solid: 50 kHz and 1 mJ

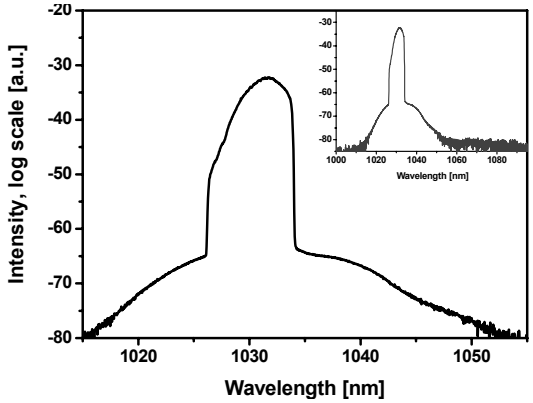

Fig.2. Spectral characteristics of the output at 1.45 mJ pulse energy; inset: larger wavelength scan

body. The core supports very few transverse modes; however, stable excitation of the fundamental mode only is achieved by seed mode matching. A power independent beam quality characterized by a M^2-value of less than 1.2 and a mode-field diameter as large as 71 µm, corresponding to an effective mode-field area of 4000 μm^2, have been measured. The fiber length used in this experiment is 1.2 m. The degree of polarization of the fiber amplifier output is 98% allowing for an efficient recompression of the pulses. The throughput efficiency of the compressor is 70%. At 200 kHz repetition rate a compressed output power of more than 100W could be reached, corresponding to pulse energy of 500 µJ. At 50 kHz and 70 mW seed power we achieved 71 W of average power with a pump power of 180 W, corresponding to 1.45 mJ energy. leading to a compressed average power of 50 W equal to pulse energy of 1 mJ. The output spectrum of the high performance fiber CPA system at the highest extracted pulse energy is shown in figure 2. Amplified spontaneous emission and intermediated (non-selected) pulses are suppressed better than 35 dB. This inset of figure 2 shows a larger wavelength scan of the spectrum excluding the onset of stimulated Raman scattering. The autocorrelation trace of the pulses at low energy and at 1 mJ is shown in Fig. 1. This reveals a wing structure growing with pulse energy, which can be attributed to the imposed nonlinear phase. The total B-integral at the highest energy is calculated to 7. The compressed pulses exhibit an autocorrelation width of 1.23 ps (equivalent to 800 fs pulse duration). The corresponding pulse peak power is approximately 1 GW.

To demonstrate the possibility of efficient nonlinear conversion, the output pulses of the laser system operating at 200 kHz repetition rate and 440 µJ pulse energy were frequency doubled in a 1 mm long BBO crystal. To achieve an intensity of 64 GW/cm² (Pp=0.5 GW, d=1mm) inside the nonlinear crystal a fused silica lens telescope was used to reduce the beam diameter to 1 mm. Efficient conversion to the second harmonic could be obtained while maintaining an excellent beam quality. The autocorrelation of the SH beam is shown in Fig. 3. The SH power was measured to be 41 W, which corresponds to 205 µJ of pulse energy.

To show the average power scaling potential of this particular fiber we built a simple cw laser cavity pumping this fiber from both ends by fiber-coupled diode lasers emitting at 976 nm. A maximum output power of more than 710W could be reached (see Fig. 4). The output increased linearly with a slope efficiency of 66 % and was just

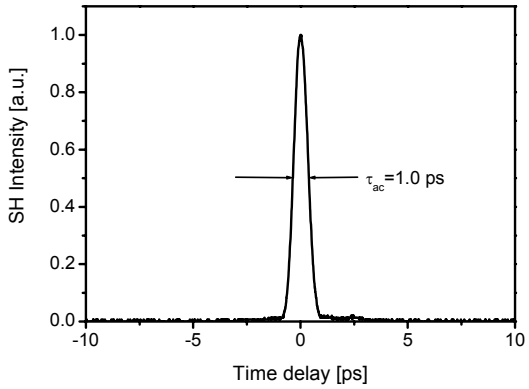

Fig.3. Measured autocorrelation trace of the SH pulses

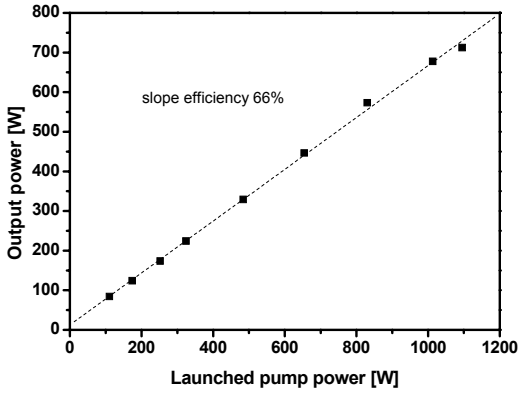

Fig.4. output chacacteristics of the cw laser cavity

pump-power limited; no roll-over was observable. This value corresponds to an extracted power per unit length of 570 W/m. Even at this high extracted power per unit length the laser operated stable, no thermal degradation occurred.

In conclusion, we have demonstrated the extraction of millijoule pulse energy femtosecond laser pulses from a fiber based CPA system at high average powers. To our knowledge, these are the highest pulse energies ever reported from a fiber based ultra-fast laser system; together with the high repetition rates this constitutes a unique performance. Key element of the system is an 80 µm core photonic crystal fiber with the ability of stable fundamental mode propagation, possessing low nonlinearity and allowing for the extraction of high average power from a short fiber length. The fiber demonstrated the capability of producing more than 710 W output power in cw operation. This shows the feasibility of a fiber based ultrashort pulse system with pulse energies above 1 mJ and average powers in the kW level.

References

1. A. Galvanauskas, G. C. Cho, A. Hariharan, M. E. Fermann, and D. Harter, "Generation of high-energy femtosecond pulses in multimode-core Yb-fiber chirped-pulse amplification systems," Opt. Lett. 26, 935-937 (2001).

2. J. Limpert, O. Schmidt, J. Rothhardt, F. Röser, T. Schreiber, A. Tünnermann, S. Ermeneux, P. Yvernault and F. Salin, “Extended single-mode photonic crystal fiber lasers,” Opt. Express 14, 2715–2720 (2006).

100 W Femtosecond Yb-Fiber CPA System based on Chirped-Volume-Bragg-Gratings

Guoqing Chang [1], Matthew Rever [1], Vadim Smirnov[2], Leon Glebov[3], and Almantas Galvanauskas [1]

[1]Department of Electrical Engineering and Computer Science, the University of Michigan, Ann Arbor, Michigan 48109-2099
[2]OptiGrate. Orlando, Florida 32826
[3]College of Optics and Photonics/CREOL, University of Central Florida, Orlando, FL
guoqingc@umich.edu

ABSTRACT

100 W amplified (75 W compressed) femtosecond (~700 fs) Yb-fiber CPA system is demonstrated using broadband chirped-volume-Bragg-gratings (CVBG) as the stretcher and compressor. With 75% compression efficiency, the CVBG based compressor exhibits an excellent average power handling capability and indicates potential for further power scaling with this compact compressor technology.
Key words: Fiber lasers, chirped-volume-Bragg-gratings

1. INTRODUCTION

Real-world applications such as THz imaging, rapid high-precision micromachining, and material processing have led to rapid advances in power scaling of Yb-fiber CPA system. The challenge to implement such a high power (>10 W) system is the development of the compressor device that can handle high average power. Therefore standard metal-coated gratings are ruled out in that they can only deal with average power below 10 W, much less than powers available from Yb-doped fiber systems. Current high power CPA technique relies on use of dielectric diffraction-grating based pulse compressors. Unfortunately such dielectric gratings still share the same critical disadvantages with the metal-coated gratings, including large size and high complexity of the optical setup with limited robustness, which offset the inherent compactness and monolithic architecture offered by fiber technology itself. Large-aperture CVBGs made of Photo-Thermo-Refractive (PTR) glasses have demonstrated capability to remove these practical limitations[1]. Incorporating CVBGs into CPA system has constituted a novel pulse stretching and compression technology that offers significant practical advantages, such as compactness, robustness, and efficiency. More importantly, CVBG based CPA compressor exhibits significant power scalability and has led to the demonstration of a 50 W Yb-doped fiber-CPA 4-ps pulse system[2] and an 8 W femtosecond (~650 fs) CPA system[3]. Here we report a significant power scaling of our previous femtosecond fiber CPA system based on 6 nm bandwidth CVBG, and demonstrate 75 W compressed ~700-fs pulses.

2. EXPERIMENTAL SETUP AND RESULTS

Figure 1 schematically illustrates the CPA system that includes an oscillator as the seed, two identical CVBGs of 2.5 cm long as the stretcher and the compressor (providing 250-ps long stretched pulses), two Yb-doped fiber amplifiers for power scaling, and two pieces of photonic band-gap fibers (PBGFs). The seed to the fiber CPA system is 110 fs pulses (centered at 1.063 μm) generated from a passively mode-locked Nd:glass oscillator operating at 72 MHz with 130 mW average power. To achieve dispersion match, two CVBGs centered at 1.063 μm with 6 nm bandwidth are arranged with opposite orientations. Both amplifiers are constructed using LMA core (30 μm core for the first stage and 65 μm for the second), double-clad Yb-doped fibers, pumped at 976 nm 940 nm respectively. The PBGFs provide an anomalous dispersion of 120 ps/nm/km at 1.063 μm in order to compensate for the normal dispersion induced by the Yb-doped fiber. Optical isolators are inserted in between to prevent feedback.

Figure 2(a) shows the dependence of the recompressed power reflected from the CVBG compressor on the incident power. Clearly the CVBG compressor has a constant efficiency of 75% and exhibits no roll-off with the incident power up to 100 W. The maximum 75 W of recompressed average power is achieved. The measured spectrum and autocorrelation trace of the recompressed pulses are plotted in Fig. 2(b) and (c). The recompressed pulse duration is estimated to be ~700 fs, about 150-fs longer than the transform-limited

pulse given by the amplified pulse spectrum. This is caused by the residual dispersion mismatch between the PBGF and the gain fiber in the current setup.

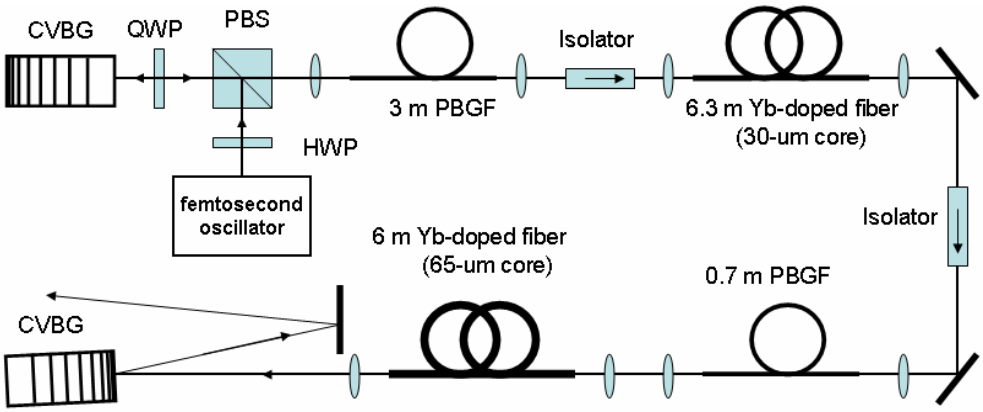

Fig. 1 Experimental setup. CVBG: chirped volume Bragg grating, HWP: half-wave plate, QWP: quarter-wave plate, PBS: polarization beam splitter, PBGF: photonic band-gap fiber

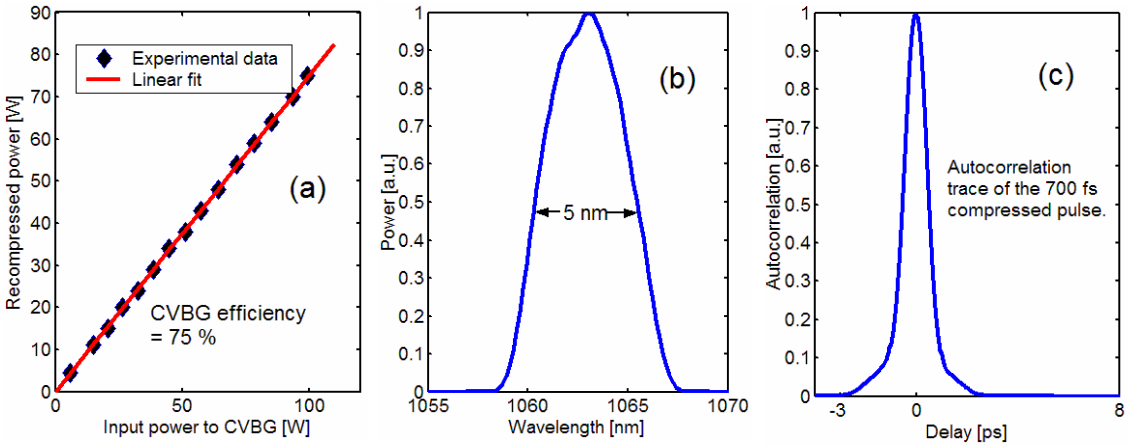

Fig. 2 (a) Compressed power of the CVBG compressor versus the incident power; (b) Spectrum of the recompressed pulse; (c) Autocorrelation trace of the recompressed pulse.

3. CONCLUSION

In conclusion, we have demonstrated a 100 W Yb-doped fiber CPA using CVBG stretchers and compressors. The independence of the 75% CVBG compression efficiency indicates good average power handling capability and implies possibility for further power scaling. These CVBGs have 6 nm bandwidths that allow the implementation of the femtosecond CPA system. It is expected that transform-limited pulses may be obtained by optimizing the PBGF length to completely compensate for the dispersion of the Yb-doped fiber. Currently, we are developing CVBGs with >10 nm bandwidths for the construction of high power fiber CPA systems with pulse durations of less than 300 fs.

References

[1] K. H. Liao, et al, "Large-aperture chirped volume Bragg grating based fiber CPA system," Optics Express 15, 4876 (2007)

[2] G. Q. Chang et al, "50-W Chirped-Volume-Bragg-Grating Based Fiber CPA at 1055-nm," paper CMEE4, CLEO/QELS, Baltimore, 2007

[3] G. Q. Chang et al, "Femtosecond Yb-Fiber CPA system based on Chirped-Volume-Bragg-Gratings," paper MD4, ASSP 2008

Stretcher-free high energy nonlinear amplification of femtosecond pulses in rod-type fiber

Y. Zaouter[1,3], D. N. Papadopoulos[2], M. Hanna[2], J. Boullet[1], L. Huang[1], F. Druon[2], E. Mottay[3], P. Georges[2], E. Cormier[1]

[1] Centre Lasers Intenses et Applications, 33405 Talence, France

[2] Laboratoire Charles Fabry de l'Institut d'Optique, CNRS, Univ Paris Sud 91127 Palaiseau France

[3] Amplitude Systèmes, 33600 Pessac, France

ABSTRACT

We report on the generation of high energy ultrashort pulses with a compact and simple stretcher-free single stage rod-type fiber amplifier in the nonlinear regime. By addition of a compact single grating compressor to compensate for the dispersion produced in the amplifier, pulses as short as 49 fs with 870 nJ pulse energy and 12 MW peak power are obtained, with a 1250 l/mm grating and higher quality pulses of 70 fs, 1.25µJ pulse energy and 16 MW peak power are generated with a 1740 l/mm grating.

Parabolic pulses are the asymptotic solution of the non-linear Schrödinger equation accounting for flat spectral gain, self phase modulation (SPM) and positive group velocity dispersion (GVD). The interplay between SPM and GVD in the presence of gain results in a wave breaking-free propagation regime [1] and the generation of purely linearly chirped amplified pulses. This linear chirp is in theory easily balanced and leads to an efficient recompression with conventional arrangement of optical elements (gratings or prisms) with negative GVD. However, this ideal asymptotic solution is experimentally largely limited due to additional deleterious effects such as a limited gain bandwidth of the fiber and the stimulated Raman scattering (SRS) [2,3]. Previous works also highlighted the impact of the Third Order Dispersion (TOD) as a restriction for such amplifiers [4,5] and the operation of parabolic amplifer beyond the gain bandwidth limit with an optimal compensation of TOD was demonstrated at record pulse peak power [6]. In this contribution we show that the direct amplification of femtoseconde pulses in short length rod-type fiber far from the optimal parabolic asymptote can lead to the generation of good quality sub-70 fs pulses at the µJ level.

The experimental setup is shown in Figure 1. The femtosecond seed source is a passively mode-locked Yb^{3+}:KYW oscillator and delivers pulses of 330 fs with a spectral bandwidth of 3.9 nm centered at 1030 nm (TBP ~ 0.36) with energy of up to 170 nJ at 10 MHz repetition rate. These pulses (up to 100 nJ) are seeded into the rod-type fiber through an optical isolator. The high power amplifier is based on an 85 cm long low-nonlinearity microstructured ytterbium-doped rod-type fiber which delivers diffraction-limited beam quality ($M^2 \sim 1.3$) out of an 80 µm core diameter. The mode field diameter of this fiber has been measured to be 70 µm (corresponding to a nonlinear parameter $\gamma=5.1\times10^{-5}$) and considerably reduces the accumulation of nonlinearities during amplification compared to conventional LMA fibers. The high numerical aperture (NA ~ 0.56) pump cladding has a diameter of 200 µm and ensures a pump absorption of 25 dB/m at 976 nm. A 100 W fiber-coupled laser diode emitting at 976 nm is used to pump the amplifier in a counter-propagating scheme. Both fiber ends are angle-polished at 8° to suppress parasitic lasing. In our setup the amplified pulses are recompressed in a two pass transmission grating-based compressor which alternatively employs two transmission gratings: a 1250 l/mm and a 1740 l/mm, both at Littrow angle of incidence i.e. 40° and 64° respectively. As they provide a considerably different TOD to Group-Velocity Dispersion (GVD) ratio of respectively -4fs and -15fs, we expected to set a different upper limit of the optimum output power level of the amplified pulses. The recompressed pulses are characterized by means of a Second Harmonic Generation Frequency Resolved Optical Gating (SHG FROG) cross-checked with independent intensity autocorrelation (50 ps delay range) and spectrometer measurements, to assure accurate identification of the pulse structure and therefore of the true peak power values obtained.

We first study the amplification and recompression of the 10 MHz pulse train to an average power of up to 10 W (1 μJ output energy) with the 1250 l/mm transmission grating based compressor. The SHG FROG retrieved intensity profiles of the seed and amplified pulses at 2W and 10W (corresponding to pulse energies after compression of 185 nJ and 870 nJ respectively) are shown in Figure 2. At 1.85 W output average power after compression the pulse duration is already dramatically reduced down to 60 fs thanks to the SPM-induced spectral broadening (inset of Figure 2). At the highest output power of 8.7 W after compression the pulse duration is shortened down to 49 fs, with FWHM time-bandwidth product (TBP) of 0.47 and RMS TBP of 3.7. However, the amount of energy contained into the main pulse peak decreases from 77% at 1.85W down to 65% at 8.7 W, due to uncompensated TOD, corresponding to an actual peak power of 2.4 MW and 12.1 MW respectively. Further increase of the output power resulted in severe distortion of the pulse structure making its characterization uncertain. In order to optimize the compensation of both the GVD and the TOD we replaced the 1250 l/mm-grating with a 1740 l/mm-grating which TOD to GVD ratio is 3.7 times larger. In Figure 4 is shown the retrieved intensity profiles in the cases of the best quality recompressed pulses, and the highest peak power pulses. For 8.5 W of amplified power (5.6 W after compression) the quality of the compressed pulses is excellent, resulting in more than 95% of the total energy contained in the 84 fs duration main pulse peak. The shortest recompressed pulses are obtained for 16 W of amplified power (10 W or 1 μJ after compression), where the pulse duration decreases down to 64 fs. The highest peak power is obtained at about 80 W of pump power resulting in 20 W output power (12.5W or 1.25μJ after compression, estimated B-integral is 8.7π) where 89% of the total energy is concentrated in the 70 fs main pulse peak (FWHM TBP of 0.58, RMS TBP of 2.4), corresponding to 16 MW peak power.

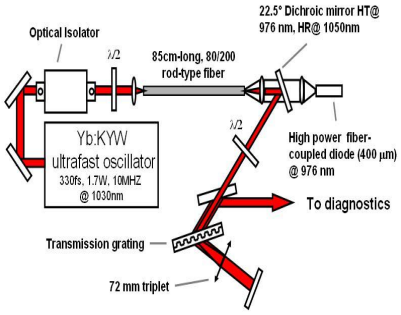

Fig1. Experimental setup

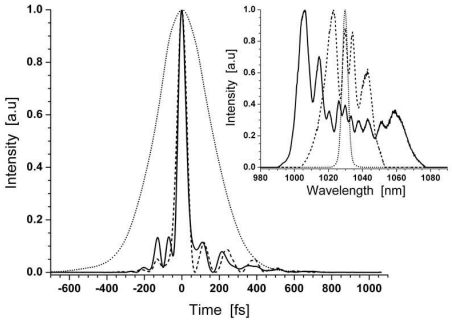

Fig2. Retrieved temporal intensity profile of the seed (dotted) and compressed pulses at 185 nJ (dashed) and 870 nJ (solid) output power (corresponding spectra in the inset) for the 1250 l/mm grating case.

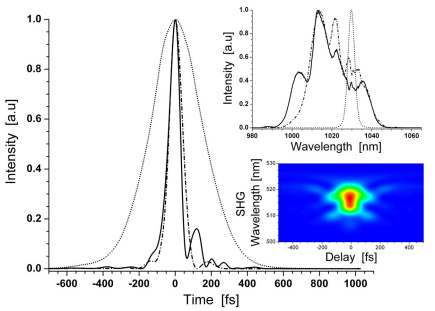

Fig3. Retrieved temporal intensity profile for the seed (dotted) and best quality recompressed pulse (dash dot), and the highest peak power pulse (solid) with corresponding spectra (top inset). (Bottom inset) SHG FROG for the highest peak power case.

In conclusion, we have demonstrated the production of 1.25μJ and 16 MW peak power pulses at 10 MHz repetition rate from a stretcher-free ytterbium-doped rod-type fiber amplifier operating in the nonlinear regime. This approach is based on direct amplification of narrowband pulses in a single-pass Ytterbium-doped rod type fiber involving embedded gain and self-phase modulation. A compact transmission grating compressor is used to compensate for the small dispersion accumulated in the amplifier. We show that the use of rod-type fibers results in peak power 4 times larger than the highest reported in a previous work [6] obtained with conventional LMA fibers.

[1] J. Limpert et al. "High-power femtosecond Yb-doped fiber amplifier," Opt. Exp. **10**, 628-638 (2002).
[2] D. Soh et al., "Efficient femtosecond pulse generation using a parabolic amplifier combined with a pulse compressor. I. Stimulated Raman-scattering effects," J. Opt.Soc. Am. B. **22**, 1-9, (2005).
[3] D. B. Soh et al. "Efficient femtosecond pulse generation using a parabolic amplifier combined with a pulse compressor. II. Finite gain-bandwidth effect," J. Opt. Soc. Am. B **23**, 10-19 (2006).

[4] Zaouter et al. “Third order phase compensation in parabolic pulse compression”, Opt. Exp. **15**, 9373-9377 (2007)
[5] Fernman et al. "Self-similar propagation and amplification of parabolic pulses in optical fibers," Phys. Rev. Lett. **84**, 6010-6013 (2000).
[6] Papadopoulos et al. "Generation of 63 fs 4.1 MW peak power pulses from a parabolic fiber amplifier operated beyond the gain bandwidth limit," Opt. Lett. **32**, 2520-2522 (2007)

A novel mode-locked fiber laser based on chirped-pulse oscillator concept

B. Ortaç, M. Plötner, T. Schreiber, J. Limpert, and A. Tünnermann

Friedrich-Schiller University, Institute of Applied Physics, Jena, Germany.

Ultra-short pulse generation has been an interesting scientific area for many decades. A number of mode-locking mechanisms in a variety of gain media has been developed making ultra-short pulse lasers to a versatile tool for many applications. In that sense fiber based mode-locked lasers have attracted considerable attention due to their inherent properties such as compactness, lack of misalignment, high efficiency and immunity against thermo-optical problems. From the scientific point of view, fiber oscillators may be likewise regarded as a very prominent example of nonlinear optical dissipative system where the nonlinear dynamics of the optical field is primarily governed by its energy exchange with the environment [1].

An intense effort is now directed toward to better control of excessive nonlinearity which typically limits the performance of fiber oscillators of nonlinearity inside mode-locked fiber laser. Power scaling of ultrashort pulse fiber-based laser system is somewhat more challenging due to nonlinear pulse distortions. This limitation can be avoided by sufficient pulse stretching in the time domain providing to reduce the peak power during the pulse amplification. The application of this technique leads to ultra-short pulse amplifier system based a Chirped-Pulse Amplification (CPA) system comprised a stretcher, a gain medium as doped fiber and a compressor unit [2]. So-called Chirped-Pulse Oscillator (CPO) concept represents a new pulse dynamic and approach of ultrashort pulse mode-locked lasers, schematic illustration of principle concept of mode-locked CPO fiber laser presented in Fig. 1, where temporal broadening phenomena is occurred by a negligible nonlinearity stretching element inside the cavity and nonlinearities could be keep under control by the pulse amplification in doped fiber. Finally, the self-consistency is principal criteria to have stable solution for mode-locked lasers and it could be achieved by the balance between the Saturable Absorber (SA) nonlinearity, stretching element and the nonlinearity into the gain fiber [3].

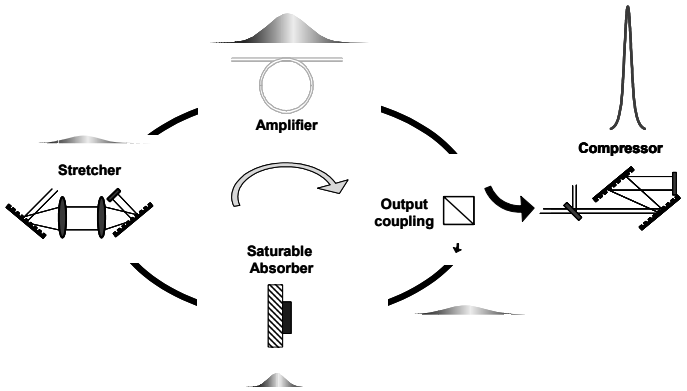

Fig. 1. Schematic illustration of principle concept of mode-locked chirped-pulse fiber laser.

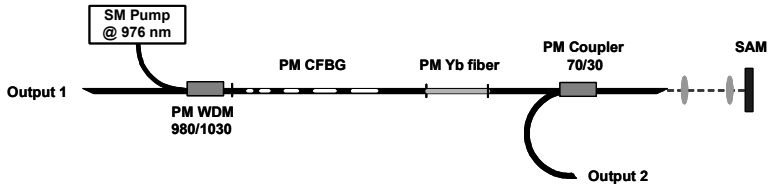

Fig. 2. Schematic experimental representation of the passively mode-locked Yb-doped polarization-maintaining chirped-pulse fiber laser. PM: polarization-maintaining; SAM: saturable absorber mirror; CFBG: chirped fiber Bragg grating.

The experimental setup of the mode-locked chirped-pulse fiber laser in a linear cavity configuration is shown in Fig. 2. As gain medium a highly ytterbium-doped polarization-maintaining (PM) single-clad fiber is used. A thin-film PM WDM is inserted outside the cavity to pump the doped fiber through the CFBG by a single-mode diode. A fiber pig-tailed thin-film 30/70 PM coupler is inserted in this configuration to study intra-cavity pulse evolution. The CFBG inscribed in a PM fiber is employed to provide positive dispersion together with negligible nonlinearity. It possesses a measured peak reflectivity of about 27% centered at 1035 nm with Gaussian-like spectral bandwidth of 16 nm (FWHM). Therefore, the CFBG serves as the output 1 of the linear cavity. The dispersion of the CFBG has been measured to be +0.19 ps^2 at 1035 nm. The passive fibers used in the setup are Panda 980 PM fibers. The output fiber end facets are angle cleaved to avoid undesired parasitic reflections or sub-cavity effects. Because of the incorporated PM fiber, the laser can be considered as environmentally stable. Self-starting passive mode-locking has been achieved by means of a semiconductor saturable absorber mirror (SAM) placed at the one end of the linear cavity. The SAM has low-intensity absorption, a high modulation depth with short relaxation time. To achieve the saturation threshold in the presented setup a telescope is used to image the output of the fiber onto the SAM. The total fiber length inside the cavity is 2 m resulting in a net-GVD of +0.286 ps^2. Hence, the laser operates in the highly positive dispersion regime, mainly caused by the CFBG.

Self-starting mode-locked operation is initiated by optimizing the saturation threshold on the SAM. At launched pump power of 130 mW, the mode-locking threshold is reached and the laser delivers a single-pulse train with a repetition rate of 44.2 MHz. We measured an average output power of 33 mW at 155 mW of pump power at output 1, which corresponds to an energy per pulse of 750 pJ. The operation of mode-locking is very stable and self-starting. Furthermore, the operation of the laser is characterized by very low amplitude noise. Figure 3(a) shows the autocorrelation trace and optical spectrum obtained in the chirped-pulse regime at output port 1. The positively-chirped output pulses present an autocorrelation width of 33.4 ps (FWHM) corresponding to a pulse duration of 21.8 ps, assuming a Gaussian pulse shape. It should be pointed out that there is no dispersion compensation element implemented intra-cavity and the pulses are always positively chirped inside the cavity. The spectrum features steep edges, which are typically observed in mode-locked fiber lasers operating in the highly positive dispersion regime. The center emission wavelength at output 1 is 1033.5 nm and the spectral bandwidth at highest pump power is 2.4 nm (10 dB) and 1.79 nm (3 dB), respectively. Figure 3(b) presents the measured autocorrelation trace of the extra-cavity compressed pulses with a pulse duration of 1.52 ps. Numerical simulation is revealed the pulses are always positively chirped inside the cavity with only one minimum located after SAM at the entrance of the fiber and pulse duration increases monotonically during the propagation in the gain and single mode fiber. We can also see the pulse stretching in the CFBG segment. Spectral filtering effects are observed in SAM due to nonlinear absorbing mechanism and CFBG due to the reflectivity properties. Finally, the self-consistency could be achieved by the balance between the SAM nonlinearity, CFBG and the nonlinearity into the gain and single mode fiber. Hence, a novel pulse generation regime of mode-locked fiber lasers has been revealed by the temporal stretching element inside the fiber oscillator. Thus, offering significantly longer average pulse duration ever reported for all-normal fiber oscillator. Hence, due to the reduced peak power scaling potential is revealed.

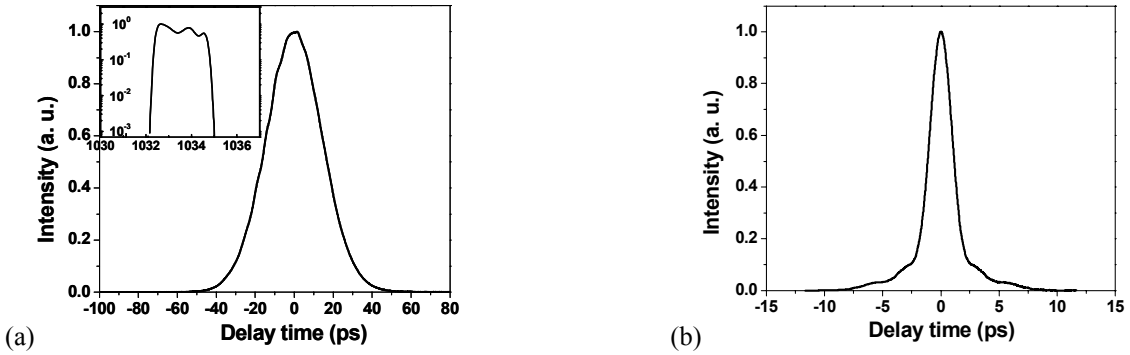

Fig. 3. (a) Autocorrelation trace of the chirped-pulses observed directly at the laser output 1. The *inset* presents the measured optical spectrum and (b) autocorrelation trace of the extra-cavity compressed pulses.

1. N. Akhmediev, and A. Ankiewicz,"Dissipative solitons," Springer-Verlag, Berlin, (2005).
2. D. Strickland and G. Mourou, Opt. Commun. 56, 219, 1985.
3. B. Ortaç, M. Plötner, J. Limpert, A. Tünnermann, Optics Express, 15, 16794, 2007.

High speed laser micro-machining using a high repetition rate, high average power femtosecond fiber CPA system

A. Ancona[1,2], K. Rademaker[1], F. Röser[1], J. Limpert[1], S. Nolte[1], A. Tünnermann[1,3]
[1]*Friedrich-Schiller-Universität Jena, Institut für Angewandte Physik, Max-Wien-Platz 1, D-07743 Jena, Germany*
[2]*CNR-INFM Regional Laboratory "LIT[3]", Dipartimento Interateneo di Fisica, via Amendola 173, I-70126 Bari, Italy*
[3]*Fraunhofer Institute for Applied Optics and Precision Engineering IOF, Albert-Einstein-Str. 7, D-07745 Jena, Germany*
Corresponding Author e-mail address: ancona@fisica.uniba.it

Abstract: We report on ultrashort pulse laser micromachining experiments on different metals at average powers up to 70 W and repetition rates up to 1 MHz. The laser pulses with subpicosecond duration were generated by an ultrafast fiber CPA laser system. The influence of particle shielding and heat accumulation on the ablation efficiency and on the processing quality will be discussed.

Laser machining has been one of the main applications of lasers since their invention. However, the precise micro-structuring especially of metallic targets is limited by thermal or mechanical damage when using conventional lasers with pulse durations in the nanosecond to microsecond regime. To overcome these limitations the use of ultrashort laser pulses for precise micro-machining has attracted much interest within the past 15 years. One of the driving applications has been the production of high aspect ratio holes. The required precision, quality and reliability are still challenging, but can be principally met using pulses with fs or ps duration, since these pulses can produce practically melting free ablation resulting in highly reproducible and well-defined holes even in metals [1]. However, one of the main drawbacks of this technique are the slow processing speeds due to the low average power and repetition rates of commercially available ultrafast laser sources, which are too low for many industrial applications. Therefore, different novel high average power ultrashort pulse laser systems have been developed in recent years, e.g. ultrafast fiber laser systems producing sub-picosecond pulses with average powers around 100 W and pulse energies of up to 1 mJ at repetition rates up to 1 MHz [2,3]. Such systems promise to overcome current limits regarding processing speed. While systematic studies on the effect of such high repetition rates on the interaction process and the resulting structures are still missing, single pulse ablation experiments with pump and probe techniques have been carried out. Based on these results an upper limit of a few hundreds kHz has been predicted for material processing with ultrashort laser pulses, before particle shielding begins to play a detrimental role [4]. In addition, the high average powers also might affect the interaction process due to heat accumulation even for ultrashort laser pulses.

In this presentation we will discuss laser drilling experiments on copper and stainless steel sheets using a novel femtosecond fiber CPA laser system operating in the parameter regime relevant for industrial applications for the first time to the best of our knowledge. The influences of repetition rate (up to 1 MHz) and average power (up to 70 Watt) on the processing time and on the resulting hole quality are investigated. Conclusions concerning heat accumulation and particle shielding will be drawn based on a simple analytical thermal model. By using a trepanning technique, we will show that is possible to produce high quality holes in 0.5 mm thick metal plates within significantly less than one second.

For the micro-machining experiments an ytterbium-doped fiber CPA system operating at a wavelength of 1030 nm has been used [2,3]. The ultrashort pulses (400 fs) are produced by a passively mode-locked Yb:KGW oscillator and temporally stretched by a dielectric grating stretcher unit. The repetition rate can be varied using an acousto-optical modulator as pulse selector. The stretched pulses are amplified in two subsequent ytterbium-doped photonic crystal fibers, both used in single-pass configuration. After compression using a dielectric grating pair, pulses of 800 fs duration, repetition rates from 25 kHz to 975 kHz and pulse energies from 10 μJ up to 70 μJ, corresponding to a maximum average power of 68.25 W at the highest repetition rate, are available. For percussion drilling experiments the laser pulses were focused with an aspheric lens (f=25 mm) onto the target surface, while a galvanometric scanning system with a 80 mm focal length F-Theta lens was used for trepanning. The samples used were high purity copper and stainless steel (Fe/Cr18Ni10) sheets with thicknesses of 0.5 and 1 mm. Laser processing times were determined by a high speed Si photodiode.

At constant pulse energies of up to 70 μJ the repetition rate has been varied from 50 kHz up to 975 kHz in order to study its influence in percussion drilling experiments on the processing time. Figure 1a summarizes the results obtained for stainless steel and the highest pulse energy investigated. The drilling time reduces significantly with repetition rate and decreases to a few ms even for a material thickness of 1 mm. More detailed information on

the ablation process can be obtained by displaying the data as the number of pulses required to breakthrough as a function of the repetition rate (exemplarily shown for a sample thickness of 0.5 mm in Fig. 1b.

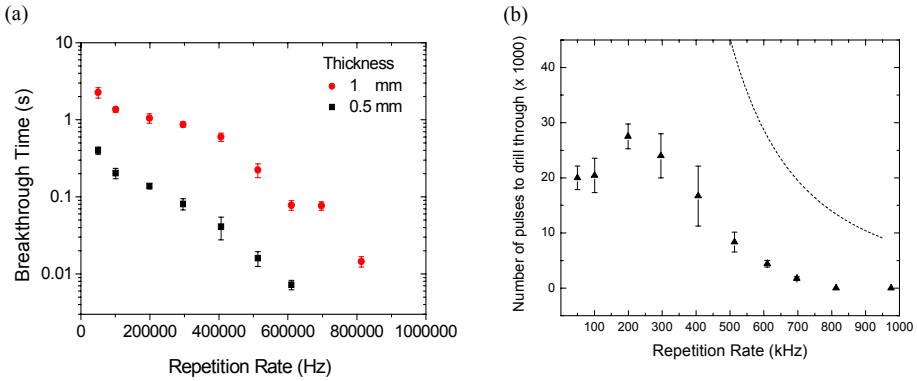

Figure 1. (a) Drilling time vs. rep. rate for 70 µJ pulse energy on 0.5-mm and 1-mm stainless steel sheets; (b) Number of pulses to breakthrough vs. rep. rate for 0.5-mm steel sheets at 70 µJ pulse energies. The dotted line represents the predicted trend due to heat accumulation.

Without particle shielding and heat accumulation a constant number of pulses could be expected to drill through the sample for a given pulse energy. However, the experimental data show that for repetition rates higher than 100 kHz the number of pulses required to drill through increases at first. This is due to particle shielding, as predicted by the single pulse pump and probe ablation experiments [4]. In contrast, a decrease of the number of pulses is observed at even higher repetition rates that can be attributed to heat accumulation occurring at the high average powers. In this case the residual thermal energy (after the ablation process) within the irradiated zone does not relax between two subsequent pulses. Consequently, the sample temperature will grow from pulse to pulse resulting in higher ablation rates and shorter drilling times. In order to visualize this effect, the dotted line in Fig. 1b represents the estimated number of pulses to reach a certain temperature (here exemplarily the melting temperature), which is obtained by solving the heat conduction equation. The experimental data points follow pretty well the trend of this curve (note that the exact position of the curve can be adjusted by assuming other temperature limits).

In contrast to these results, neither particle shielding nor heat accumulation effects were observed in case of copper samples, probably due to the higher thermal conductivity. This allows to laser trepan melt-free and high quality holes on 0.5-mm-thick copper sheets at the highest average power available, resulting in a process time of only 75 ms (Fig. 2).

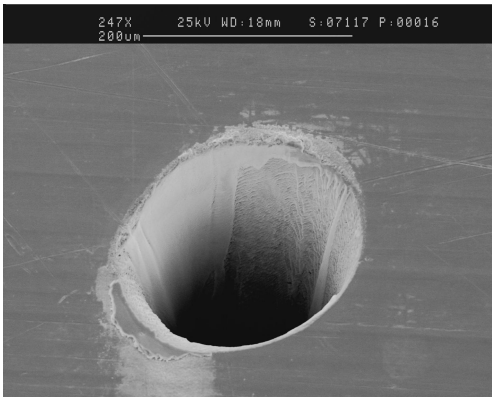

Figure 2. SEM image of laser trepanned hole in 0.5-mm copper sample (pulse energy 50 µJ, repetition rate 975 kHz, breakthrough time 75 ms).

In conclusion, ultrashort pulse laser drilling experiments have been performed on metals at high repetition rates up to the MHz regime. Processing times have been reduced to a few ms, demonstrating great potential for industrial applications. Depending on the thermal properties of the samples investigated the influence of particle shielding on the processing speed could be observed. At even higher repetition rates this effect is compensated by heat accumulation. Both mechanisms are negligible for high thermal conductivity materials like copper, where high quality melt-free and holes have been drilled using a trepanning technique within few tens of ms.

References

1. B.N. Chichkov et al., "Femtosecond, picosecond and nanosecond laser ablation of solids", Appl. Phys. A **63**, 109 – 115 (1996)
2. F. Röser, at al., "90 W average power 100 µJ energy femtosecond fiber chirped-pulse amplification system", Opt. Lett. 32, 2230-2232 (2007)
3. F. Röser, et al., "Millijoule pulse energy high repetition rate femtosecond fiber chirped-pulse amplification system", Opt. Lett. 32, 3495-3497 (2007)
4. J. König at al., "Plasma evolution during metal ablation with ultrashort laser pulses", Opt. Exp. **13** (26) 10597-10607 (2005)